Utah Energy Balance Snow Accumulation and Melt Model (UEB)

David G. Tarboton
Charles H. Luce

Computer model technical description and users guide.

This program was written and prepared under agreement with and funding by the U.S. Government , and therefore is in the public domain and not subject to copyright.

Prepared through a co-operative agreement between

Utah Water Research Laboratory
Utah State University

and

USDA Forest Service
Intermountain Research Station

December 1996

TABLE OF CONTENTS

Preface (i)
Acknowledgements (i)

Abstract 1

Section 1. Technical Description 2
- Introduction 2
- Literature review 2
- Model Description 6
  - Shortwave radiation and albedo 9
  - Longwave radiation 12
  - Snow fall accumulation and heat with precipitation 13
  - Turbulent fluxes 14
  - Snow surface temperature 16
  - Meltwater Outflux 17
  - Forest cover 17
- Calibration and Testing 18
  - Central Sierra Snow Laboratory - calibration 18
  - Reynolds Creek Experimental Watershed - testing 19
  - USU drainage and evapotranspiration research farm - testing 20
  - Mammoth Mountain - testing 22
- Conclusions 23

Section 2. Guide to using the model (UEB) 24

References 33

Figure captions and figures 39

Preface

This work is part of a project involving a series of collaborative agreements between the USDA Forest Service Intermountain Research Station and Utah State University. The overall objective of this project was to develop procedures for generating weather and surface water inputs (mountain climate generator, MCLIGEN) for use in the WEPP (*Lane and Nearing*, 1989) erosion model that the USFS is currently adapting to suit their needs in the mountainous regions of the western U.S. Since snowmelt comprises a large fraction of the surface water input in these regions the ability to model snowmelt was required. This work describes the snowmelt model developed for these purposes.

The model is available electronically on the internet by anonymous ftp from fox.cee.usu.edu or by contacting David Tarboton (dtarb@cc.usu.edu http://www.engineering.usu.edu/dtarb/). The distribution package is available in UNIX tar format and DOS zip format and includes the source code, make file (UNIX version), executable (DOS version), and example input and output files.

Acknowledgements

This model was developed with support from the USDA Forest Service through a series of Resource Joint Venture Agreements and the U.S. Department of the Interior, Geological Survey, under USGS Grant No. 14-08-0001-G2110, Utah State University through a faculty research grant and the Utah Water Research Laboratory. I am grateful to these sponsors for this support. I am grateful to the following colleagues and students who participated in this project; David Bowles, Upmanu Lall, Gail Bingham, Tom Jackson, Tanveer Choudhury, Mohammed Al-Adhami. Bruce McGurk provided and helped with interpretation of the Central Sierra Snow Laboratory data; thank you. Thanks also to Keith Cooley and the USDA ARS Northwest Watershed Research Center staff for access to and collaboration in Reynolds Creek. Thank you Richard Allen for access to the USU drainage and evaporation research farm instrumentation, data and assistance in instrumentation setup and data reduction. Thank you Arijit Chattopadhyay for your efforts as field assistant.

The views and conclusions presented are those of the authors and should not be interpreted as necessarily representing the official policies, either expressed or implied, of the U.S. government or sponsoring agencies.

Abstract

An energy balance snowmelt model was developed for the prediction of rapid snowmelt rates potentially responsible for soil erosion and surface water inputs. The model uses a lumped representation of the snowpack with two primary state variables, namely, water equivalence and energy content relative to a reference state of water in the ice phase at 0 ^{o}C. This energy content is used to determine snowpack average temperature or liquid fraction. Snow surface age is retained as a third state variable, used for the calculation of albedo. The model is driven by inputs of air temperature, precipitation, wind speed, humidity and radiation at time steps sufficient to resolve the diurnal cycle (hourly or six hourly). The model uses physically-based calculations of radiative, sensible, latent and advective heat exchanges. An equilibrium parameterization of snow surface temperature accounts for differences between snow surface temperature and average snowpack temperature without having to introduce additional state variables. Melt outflow is a function of the liquid fraction, using Darcy's law. This allows the model to account for continued outflow even when the energy balance is negative. Because of its parsimony (only three state variables) this model is suitable for application in a distributed fashion on a grid over a watershed. This report gives a detailed description of the model, together with results of tests against data collected at the Central Sierra Snow Laboratory, California; Reynolds Creek Experimental Watershed, Boise Idaho; and at the Utah State University drainage and evapotranspiration research farm, Logan Utah. The testing includes comparisons against melt outflow collected in melt lysimeters, surface snow temperatures collected using infrared temperature sensors and depth and water equivalence measured using snow core samplers. This report also provides instructions for using the model.

I. TECHNICAL DESCRIPTION

Introduction

Snowmelt is a significant surface water input of importance to many aspects of hydrology including water supply, erosion and flood control. Snowmelt is driven primarily by energy exchanges at the snow-air interface. The model described herein was developed initially to predict the rapid melt rates responsible for erosion. It has also been used to provide the spatially distributed surface water input in a water balance study. In developing a new snowmelt model our goal was to incorporate ideas from the many existing models and parameterize the processes involved in as simple, yet physically correct a manner as possible. We hoped to develop a parsimonious, physically-based model that could be driven by readily available inputs and applied anywhere with no (or minimal) calibration. The striving for simplicity led us to parameterize a snowpack in terms of lumped (depth averaged) state variables so as to avoid having to model the complex processes that occur within a snowpack. We have still, however, attempted to capture important physical differences between bulk (depth averaged) properties and the surface properties that are important for surface energy exchanges.

In the remainder of this report we first review literature, highlighting current understanding of snow and snowmelt processes. We then describe the model developed. Tests of the model against data from the Central Sierra Snow Laboratory, California; Reynolds Creek Experimental Watershed, Boise Idaho; and the Utah State University drainage and evapotranspiration research farm, Logan Utah are then presented. These demonstrate the effectiveness and some shortcomings of the model. We then provide a guide to using the model and information on obtaining it.

Literature Review

We have relied heavily on an understanding of snowmelt processes gleaned from Gray and Male (1981) and the descriptions of existing models (*Anderson*, 1973; 1976; *Morris*, 1982; *Leavesley et al*., 1983; *Kondo and Yamazaki*, 1990).

The basic understanding of snow hydrology has evolved over the past 35 years, starting with the report *Snow Hydrology* (*U.S. Army Corps of Engineers*, 1956) and is now described in most introductory hydrology texts (*Linsley et al*., 1975; *Viessman et al*., 1989; *Bras*, 1990; *Dingman*, 1994). The physical processes within a snowpack and involved in snowmelt are highly complex, involving mass and energy balances as well as heat and mass transport by conduction, vapor diffusion and meltwater drainage. There is also formation of ice layers which impede the downward propagation of infiltrating meltwater resulting in concentrated finger flow and sometimes lateral flow. Colbeck (1978; 1991) reviews these issues. Here we only summarize the

processes pertinent to our work.

Figure 1 illustrates the energy exchanges important in snowmelt and snowpack ablation. Typical data (e.g. *Male and Gray,* 1981) indicates that the radiation fluxes are usually larger than sensible and latent heat fluxes which are in turn larger than fluxes to the ground.

Radiative heat transfers consist of absorption and reflection of incoming solar (shortwave) radiation as well as absorption and emission of longwave radiation. Radiative energy inputs are the most important energy exchange mechanism for snowmelt (*Male and Gray*, 1981). Incoming solar radiation is a function of latitude, season, aspect, slope and radiative transmissivity of the atmosphere as well as weather conditions such as clouds. Apart from the effect of clouds the other factors are predictable. In mountain regions terrain shading plays an important role in the amount of radiation reaching a given point. (*Dozier*, 1979) describes a complete solar radiation model which includes a shading function. The reflection of solar radiation is described in terms of the albedo which can vary considerably as a function of the condition and age of the snow surface. Given the magnitude of the solar radiation term in the energy balance modest albedo changes are important to the snow surface energy balance. The albedo of snow is generally maximum after a fresh snowfall and decreases with time due to growth in grain sizes, melt water near the snow surface and the accumulation of dust and debris on the snow surface (*U.S. Army Corps of Engineers*, 1956). The rate of grain growth is a function of surface temperature (*Wiscombe and Warren*, 1981; *Dozier*, 1987; *Marshall and Warren*, 1987).

Incoming longwave radiation is essentially black body radiation from the atmosphere, and is often modeled as a function of surface air temperature with emissivity parameterized as a function of vapor pressure. Several parameterizations are available (*Brunt*, 1952; *Kuz'min*, 1961; *Brutsaert*, 1975; *Marks and Dozier*, 1979; *Satterlund*, 1979). These generally work best for clear skies and are not recommended for cloudy conditions. Price and Dunne (1976) note some problems associated with using near surface measurements to characterize the vertical distribution of air mass properties.

Outgoing longwave radiation is also black body radiation from the snow surface with an emissivity usually between 0.97 and 1 (*Anderson*, 1976). Night time longwave radiation losses under clear skies are responsible for considerable cooling of the snow surface. However actual heat loss is limited by the small thermal conductivity of the snow. In areas of high relief the atmospheric radiation received at a point, e.g. in a valley is reduced because part of the sky is obscured by the adjacent mountains. However scattered and emitted radiation from mountain side slopes is present. Procedures for computation of horizon angles and sky and terrain view factors should be used to account for these effects (*Dozier*, 1979; *Dozier and Frew*, 1990; *Dubayah et al.*, 1990; *Frew*, 1990).

Turbulent energy transfers comprise sensible and latent heat fluxes. Sensible heat fluxes depend on the temperature gradient and turbulent diffusion due to wind. Latent heat fluxes comprise evaporation and condensation of liquid water and sublimation of ice and occur at the surface at a rate controlled by the vapor pressure gradient and turbulent diffusion in the overlying air (*Male and Gray*, 1981; *Bras*, 1990). As well as removing water these processes cool the snowpack by removal of latent heat. One unit of evaporation can freeze 7.5 units of liquid water (*Bras*, 1990). The turbulent diffusion is controlled by surface roughness and the log profile of wind velocity with height. The magnitude of these effects underscores the importance of wind and atmospheric humidity and the difference between open and forested areas. Turbulent transfer rates also depend on atmospheric stability which is a function of the temperature gradients. Brutsaert (1982) reviews the similarity theory and adjustments required for stability/instability effects. In the context of snow stability/instability is also discussed by Male and Gray (1981) and Price and Dunne (1976).

At the base of the snowpack there are energy exchanges with the soil and melt water percolation which forms infiltration or runoff depending on the underlying soil conditions. Ground heat flux is generally much smaller than the surface energy transfers (*Bras*, 1990) and is frequently neglected over short time periods. However the integrated affect over a season can be significant (*Male and Gray*, 1981). In early season even short periods are affected by ground heat flux.

Melt is generally considered to occur at or near the snow surface because that is where most of the energy available for melt arrives. Anderson (1968) reports that 80% of solar radiation is absorbed in the top 5-15 cm of a snow pack, dependent on density. The surface also receives any new snow or rain, which can bring with it significant energy.

Vegetation, especially forest cover, affects the distribution of snow (*Kuz'min*, 1961; *McKay and Gray*, 1981; *Troendle and Leaf*, 1981; *Gary and Troendle*, 1982; *Toews and Guns*, 1988). One of the conclusions of the World Meteorological Organization (1986) study was that the effect of vegetation on interception was important, especially when trying to forecast the effect of land use changes. There seems to be general agreement (*Troendle and Leaf*, 1981; *Gary and Troendle*, 1982; *Toews and Guns*, 1988) that trees through their affect on boundary layer wind patterns influence the accumulation of snow. McKay and Gray (1981) discuss this issue in detail, noting the following factors that affect the distribution of snow at different scales:

- Macroscale: (10^4 - 10^5 m) Elevation, orography, meteorological effects such as standing waves, flow of wind around barriers and lake effects.
- Mesoscale: (10^2-10^3 m) Redistribution due to wind and avalanches, deposition and accumulation related to elevation, slope, aspect, vegetative cover height and density.
-Microscale: (10-10^2 m) Primarily surface roughness and transport phenomena.

From the above discussion it can be seen that the major state variables which characterize snowpack are water equivalence, depth, vertical temperature and density profiles, and albedo and liquid water content. Many snowmelt models have been developed to describe the evolution of these variables. Some of those we reviewed included the Stanford watershed model snow components (*Anderson and Crawford*, 1964); National Weather Service River Forecast System (NWSRFS) - Snow Accumulation and Ablation model (*Anderson*, 1973); The Utah State University simulation model (*Riley et al*., 1966); Anderson point energy and mass balance model (*Anderson*, 1976), snow components of the SHE model (*Morris*, 1982); the U.S.G.S. Precipitation-Runoff Modeling System (PRMS), (*Leavesley et al.*, 1983; 1987) and the existing WEPP snowmelt subroutines (*Hendrick et al.*, 1971; *Young et al.*, 1989). Levels of implementation of models range from 1) Index related methods, through 2) Energy Budget methods and 3) Full solutions of the equations of flow of energy and mass. The SHE model (*Morris*, 1982), has implementations at all these levels of detail dependent on the information available. The Utah State University simulation model (*Riley et al*., 1966; *Leu*, 1988) is a hybrid containing elements from all three levels. The Stanford watershed model uses a combination of energy budget and index methods (*Anderson*, 1968). The NWSRFS model uses index related methods during dry melt periods, but an energy budget approach for melt during rain. Anderson's point energy balance model (*Anderson*, 1976) is a detailed solution to the mass and energy flow equations using finite difference techniques. The PRMS snow component maintains energy and water balances assuming a two layer system (*Leavesley et al.*, 1987). The WEPP snowmelt component (*Young et al.*, 1989) is based on the Hendrick equation and amounts to a physically derived index equation dependent on temperature, radiation and precipitation inputs.

In developing a model one needs to keep in mind that the level of sophistication chosen should be consistent with the input data. Charbonneau et al. (1981) tested different snowmelt runoff models in an alpine basin in France and concluded that the choice of interpolation procedures for input data such as air temperature and precipitation is much more crucial than the level of sophistication of individual snowmelt models.

Recently the World Meteorological Organization (1986) compared 11 different snowmelt runoff models from several countries. Most of the models were at a basin scale, i.e. too large a scale for use here, but their relevant conclusions were:
- Most models used a temperature index approach, with monthly melt factor.
- It is important to suppress melt during the ripening period, to account for the cold content and liquid water storage.
- Subdivision of basins into elevation zones is important.
- Further work on lapse rates is necessary
- The interception of snow is important especially to forecast the effect of land use changes.

In the model we developed, described next, we have drawn on ideas from many of these models

and studies.

Model Description

Our model design goals were:
• Simplicity. Small number of state variables and adjustable parameters.
• Physically based, so that the model is transportable and applicable without calibration at different locations.
• Match diurnal cycle of melt outflow rates for erosion prediction.
• Match overall accumulation and ablation for water balance.
• Distributed by application over a spatial grid.

Figure 2 depicts schematically the model physics and parameterizations. The snowpack is characterized by three state variables, water equivalence W [m], energy content U [kJ m^{-2}], and the age of the snow surface which is only used for albedo calculations. Water equivalence includes any liquid water present in the snowpack. W and U are defined per unit of horizontal area. These are, we believe, sufficient to characterize the snowpack for the surface water inputs of interest. The state variable, energy content U, is defined relative to a reference state of water at 0°C in the ice (solid) phase. U greater than zero means the snowpack (if any) is isothermal with some liquid content and U less then zero can be used to calculate the snowpack average temperature T [°C]. Energy content is defined as the energy content of the snowpack plus a top layer of soil with depth D_e [m]. We discuss below the choice of D_e and the role it plays in the model.

The model is designed to be driven by inputs of air temperature T_a [°C], wind speed V [m s^{-1}], relative humidity RH, precipitation P [m hr^{-1}], incoming solar Q_{si} and longwave Q_{li} radiation [kJ $m^{-2}hr^{-1}$], and ground heat flux Q_g [kJ $m^{-2}hr^{-1}$] (taken as 0 when not known) at each time step. The time step should be sufficient to resolve the diurnal cycle in energy inputs. Time steps of 0.5, 1 and 6 hours have been used in data comparisons here. When incoming solar radiation is not available it is estimated as an extra-terrestrial radiation (from sun angle and solar constant) times an atmospheric transmission factor T_f, estimated from the daily temperature range using the procedure given by Bristow and Campbell (1984). When incoming longwave radiation is not available it is estimated based on air temperature, the Stefan-Boltzman equation and a parameterization of air emissivity due to Satterlund (1979), adjusted for cloudiness using T_f.

Given the state variables U and W, their evolution in time is determined by solving the following energy and mass balance equations.

$$\frac{dU}{dt} = Q_{sn} + Q_{li} + Q_p + Q_g - Q_{le} + Q_h + Q_e - Q_m \quad (1)$$

$$\frac{dW}{dt} = P_r + P_s - M_r - E \quad (2)$$

In the energy balance equation (all per unit of horizontal area i.e. in kJ $m^{-2}hr^{-1}$) terms are: Q_{sn}, net shortwave radiation; Q_{li}, incoming longwave radiation; Q_p, advected heat from precipitation; Q_g, ground heat flux; Q_{le}, outgoing longwave radiation; Q_h, sensible heat flux; Q_e, latent heat flux due to sublimation/condensation; and Q_m, advected heat removed by meltwater. In the mass balance equation (all in m/hr of water equivalence) terms are: P_r, rainfall rate; P_s, snowfall rate; M_r, meltwater outflow from the snowpack; and E, sublimation from the snowpack. Many of these fluxes depend functionally on the state and input driving variables. We elaborate on the parameterization of these functional dependencies below.

The use of energy content as a state variable means that the model does not explicitly prognose snowpack temperature. Since snowpack temperature is a quantity important for energy fluxes into the snow it needs to be obtained diagnostically from the state variables energy content, U, and water equivalence, W, as follows, recalling that U is defined relative to 0˚C ice phase.

If $U < 0$	$T = U/(\rho_w W C_s + \rho_g D_e C_g)$	All solid phase	(3)
If $0 < U < \rho_w W h_f$	T = 0˚C.	Solid and liquid mixture	(4)
If $U > \rho_w W h_f$	$T = \frac{U - \rho_w W h_f}{\rho_g D_e C_g + \rho_w W C_w}$	All liquid	(5)

In the above the heat required to melt all the snow water equivalence at 0 ˚C is $\rho_w W h_f$ [kJ m^{-2}] where h_f is the heat of fusion [333.5 kJ kg^{-1}] and U in relation to this determines the solid-liquid phase mixtures. The heat capacity of the snow is $\rho_w W C_s$ [kJ $˚C^{-1}$ m^{-2}] where ρ_w is the density of water [1000 kg m^{-3}] and C_s the specific heat of ice [2.09 kJ kg^{-1} $˚C^{-1}$]. The heat capacity of the soil layer is $\rho_g D_e C_g$ [kJ $˚C^{-1}$ m^{-2}] where ρ_g is the soil density and C_g the specific heat of soil. These together determine the T when $U < 0$. Practically in (5) W is always 0, since a completely liquid snowpack cannot exist. Nevertheless this equation is included for completeness to keep track of energy content during periods of intermittent snow cover. The heat capacity of liquid water, $\rho_w W C_w$, where C_w is the specific heat of water [4.18 kJ kg^{-1} $˚C^{-1}$], is included for numerical consistency during time steps when the snowpack completely melts. When there is a solid and liquid phase mixture the liquid fraction $L_f = U/(\rho_w h_f W)$ quantifies the mass fraction of total snowpack (liquid and ice) that is liquid.

The parameter D_e is intended to quantify the depth of soil that interacts thermally with the snowpack. Heat flow in snow and soil is governed by Laplace's equation. The depth of penetration of changes in surface temperature can be evaluated from the expression (*Rosenberg,* 1974):

$$\frac{R_z}{R_s} = \exp\left(-z\left(\frac{\pi}{\alpha P}\right)^{\frac{1}{2}}\right) \tag{6}$$

where R_s, is the range of temperature oscillation at the surface; R_z, the range of temperature oscillation at depth z; P, the period of oscillation; and α, the thermal diffusivity. For soil α is typically in the range 0.0014 to 0.0022 $m^2\ hr^{-1}$. Figure 3 shows R_z/R_s versus z for α = 0.0018 $m^2\ hr^{-1}$ for various periods. This figure shows that for oscillations with period less than one week the effect at 0.4 m is damped to less than 30% and even for monthly oscillations is still damped 50% at 0.4 m depth. This result suggests using D_e = 0.4 m in our model since the time scale of interest is the seasonal accumulation then melting of snow. The state variable U represents energy content above this level. The ground heat flux represents heat transport at this depth and is therefore a long-term average. High frequency oscillating ground heat fluxes above this depth are absorbed into U, the energy stored in the snow and soil above depth D_e. This procedure provides a simple approximation of the effects of frozen ground, or snow falling on warm ground.

Equations (1) and (2) form a coupled set of first order, nonlinear ordinary differential equations. They can be summarized in vector notation as:

$$\frac{d\underline{X}}{dt} = \underline{F}(\underline{X}, \text{driving variables}) \tag{7}$$

where $\underline{X}$ = (U, W) is a state vector describing the snowpack. With $\underline{X}$ specified initially, this is an initial value problem. A large variety of numerical techniques are available for solution of initial value problems of this form. Here we have adopted an Euler predictor-corrector approach (*Gerald,* 1978).

$$\underline{X}' = \underline{X}_i + \Delta t\, \underline{F}(\underline{X}_i, \text{driving variables}) \tag{8}$$

$$\underline{X}_{i+1} = \underline{X}_i + \Delta t\, \frac{\underline{F}(\underline{X}_i, \text{driving variables}) + \underline{F}(\underline{X}', \text{driving variables})}{2} \tag{9}$$

where Δt is the time step, $\underline{X}_i$ refers to the state at time t_i and $\underline{X}_{i+1}$ refers to the state at time $t_{i+1}=t_i+\Delta t$. This is a second order finite difference approximation, with global error proportional to Δt^2 (*Gerald*, 1978, p257). Numerical instabilities sometimes occur under melting conditions when the snowpack is shallow due to the nonlinear nature of the melt outflow parameterization. To deal with this we compare $\underline{X}_{i+1}$ to $\underline{X}'$ and if they differ by more than a specified tolerance (0.025 m for W and 2000 kJ/m^2 for U) we iterate up to four times setting $\underline{X}'$ to $\underline{X}_{i+1}$ then recalculating $\underline{X}_{i+1}$ at each iteration. If convergence is still not achieved we take the solution that would keep the liquid fraction of the snow constant.

In the following we describe how each of the processes involved in equations (1) and (2) are parameterized.

Shortwave Radiation and Albedo

Net shortwave radiation is calculated as:

$$Q_{sn} = Q_{si} (1-A) \tag{10}$$

where A is albedo and Q_{si} incident shortwave radiation either measured on site or estimated from diurnal temperature range (*Bristow and Campbell*, 1984). Albedo is calculated as a function of snow surface age and solar illumination angle following Dickinson et al. (1993, p21.).

Incident shortwave (solar) radiation is taken as:

$$Q_{si} = T_f \cdot I_o \cdot HRI \tag{11}$$

Here I_o is the solar constant (4914 kJ m^{-2} hr^{-1}), T_f an atmospheric transmittance and HRI a multiplication factor based on the integral of the illumination angle over the time step:

$$HRI = \frac{1}{\cos(\theta)\,\Delta t} \int_t^{t+\Delta t} \cos(\psi)\, dt \tag{12}$$

The $\cos(\theta)$ in the denominator is the cosine of the local slope included because radiation flux is defined per unit horizontal area. This integral is evaluated using the concept of equivalent slope (e.g. *Riley et al.*, 1966; or *Dingman*, 1994) to account for the dependence of the position of the sun on season, latitude and time of day and adjust for slope and aspect.

When solar radiation is measured on site (with horizontally mounted pyranometers) the measured radiation Q_m is used to infer T_f with from the radiation multiplication factor calculated with slope specified as 0, denoted HRI_0.

$$T_f = Q_m/(I_o\ HRI_0) \tag{13}$$

Substituting this into equation (11) results in:

$$Q_{si} = Q_m\ HRI/HRI_0 \tag{14}$$

which effectively adjusts horizontally measured radiation to a sloping surface.

If measured incident solar radiation is unavailable it is estimated using equation (11) with the atmospheric transmittance factor obtained using the procedure of Bristow and Campbell (1984):

$$T_f = a\ [1-\exp(-b\Delta T^c)] \tag{15}$$

where ΔT is the diurnal temperature range and a (=0.8) and c (=2.4) are parameters that Bristow and Campbell calibrated. b is a parameter dependent on the monthly mean diurnal temperature range $\overline{\Delta T}$.

$$b = 0.036\ \exp(-0.154\ \overline{\Delta T}) \tag{16}$$

The constants in these equations were calibrated based on the particular data and location Bristow and Campbell used. However checks against measurements of solar radiation at the Central Sierra Snow Lab and Utah State University suggest they are transferable between locations.

Albedo is calculated as a function of snow surface age and solar illumination angle following Dickinson et al. (1993, p21.). The age of the snow surface is retained as a state variable, and is updated with each time step, dependent on snow surface temperature and snowfall. Reflectance is computed for two bands; visible (< 0.7 μm) and near infrared (> 0.7 μm) with adjustments for illumination angle and snow age. Then albedo is taken as the average of the two reflectances:

$$\alpha_{vd} = (1-C_v\ F_{age})\alpha_{vo} \tag{17}$$

$$\alpha_{ird} = (1-C_{ir}\ F_{age})\alpha_{iro} \tag{18}$$

Here α_{vd} and α_{ird} represent diffuse reflectances in the visible and near infrared bands

respectively. F_{age} is a function to account for aging of the snow surface. C_v (= 0.2) and C_{ir} (=0.5) are parameters that quantify the sensitivity of the respective band albedo to snow surface aging (grain size growth), and α_{vo} (=0.85) and α_{iro} (=0.65) are fresh snow reflectances in each band. F_{age} is given by:

$$F_{age} = \tau/(1+\tau) \tag{19}$$

where τ is a non-dimensional snow surface age that is incremented at each time step by the quantity designed to emulate the effect of the growth of surface grain sizes:

$$\Delta\tau = \frac{r_1+r_2+r_3}{\tau_o}\,\Delta t \tag{20}$$

Here Δt is the time step in seconds with $\tau_o = 10^6$ s. r_1 is a parameter dependent on snow surface temperature, T_s [˚K], intended to represent the effect of grain growth due to vapor diffusion.

$$r_1 = \exp[5000\,(\frac{1}{273.16} - \frac{1}{T_s})] \tag{21}$$

r_2 represents the additional effect near and at freezing point due to melt and refreeze:

$$r_2 = \min(r_1^{10}, 1) \tag{22}$$

r_3 = 0.03 (0.01 in Antarctica) represents the effect of dirt and soot.

0.01 m of snowfall is assumed to restore the snow surface to new conditions (τ = 0). With snowfall, P_s, less than 0.01 m in a time step the dimensionless age is reduced by a factor ($1-100P_s$)

The reflectance of radiation with illumination angle ψ (measured relative to the surface normal) is computed as

$$\alpha_v = \alpha_{vd} + 0.4\, f(\psi)(1-\alpha_{vd}) \tag{23}$$

$$\alpha_{ir} = \alpha_{ird} + 0.4\, f(\psi)(1-\alpha_{ird}) \tag{24}$$

where

$$f(\psi) = \frac{1}{b}\left[\frac{b+1}{1+2b\cos(\psi)} - 1\right] \quad \text{for } \cos(\psi) < 0.5$$
$$= 0 \quad \text{otherwise} \tag{25}$$

where b is a parameter set at 2 by Dickinson et al. (1993, p21.). The above equation increases reflectance for illumination angles larger than 60˚. When the snowpack is shallow (depth $z < h = 0.1$ m) the albedo is taken as $r A_{bg} + (1-r) A$ where $r = (1-z/h)e^{-z/2h}$. This interpolates between the snow albedo and bare ground albedo (A_{bg}) with the exponential term approximating the exponential extinction of radiation penetration of snow.

Longwave Radiation

Outgoing longwave radiation is

$$Q_{le} = \varepsilon_s \sigma T_s^4 \tag{26}$$

where ε_s is emissivity, σ the Stefan Boltzmann constant [2.07×10^{-7} kJ m^{-2} hr^{-1} ˚K^{-4}] and T_s is absolute temperature [K].

Incoming longwave radiation is intended to be a model input. However where this is not available it is estimated based on air temperature (T_a in ˚K) using the Stefan-Boltzmann equation

$$Q_{li} = \varepsilon_a \sigma T_a^4 \tag{27}$$

with air emissivity (ε_a) based on air vapor pressure (e_a in Pa), air temperature (T_a in kelvin) and cloud cover. We use the Satterlund (1979) parameterization of emissivity for clear sky conditions:

$$\varepsilon_{acls} = 1.08\left[1 - \exp\left(-\left(\frac{e_a}{100}\right)^{T_a/2016}\right)\right] \tag{28}$$

This is adjusted for the cloud cover fraction which is estimated from the Bristow and Campbell (1984) transmission factor

$$CF = 1\text{-}T_f/a \tag{29}$$

This is based on the notion that under clear skies T_f will approach its maximum value "a", but be reduced below "a" as cloudiness increases. We then use:

$$\varepsilon_a = CF + (1\text{-}CF)\varepsilon_{acls} \tag{30}$$

in equation (27) to estimate incoming longwave radiation.

Snow fall accumulation and heat with precipitation

Measured precipitation rate P, is partitioned into rain P_r, and snow P_s, (both in terms of water equivalence depth) using the following rule based on air temperature T_a, (*U.S. Army Corps of Engineers*, 1956)

$$\begin{array}{ll} P_r = P & T_a \geq T_r = 3\ ^oC \\ P_r = P(T_a - T_b)/(T_r - T_b) & T_b < T_a < T_r \\ P_r = 0 & T_a \leq T_b = -1\ ^oC \end{array} \tag{31}$$

$$P_s = (P - P_r)\, F \tag{32}$$

where T_r is a threshold air temperature above which all precipitation is rain and T_b a threshold air temperature below which all precipitation is snow. The accumulation of snow is sometimes subject to considerable wind redistribution with drifts forming on lee slopes. We account for this in the model through a snow drift factor, F, dependent on location (*Jackson*, 1994; *Jackson et al.*, 1996). Ideally F needs to be related to topography. In the application to Reynolds Creek, F was estimated by calibrating the snow water equivalences obtained from the snow model at each cell, W_m, against the observed values, W_o. The discrepancy between observations and predictions over an interval between measurements is attributed to drifting and F adjusted until W_m equals W_o at the end of the interval. Values of F less than one correspond to locations of depletion or wind scour. This approach models drifting which actually occurs after snowfall as concurrent with snowfall. The calibration of F assumes that the snowmelt model correctly accounts for all other processes (melt, sublimation, condensation, etc.) affecting the accumulation and ablation of snow water equivalence.

The temperature of rain is taken as the greater of the air temperature and freezing point and the temperature of snow is the lesser of air temperature and freezing point. The advected heat is the energy required to convert this precipitation to the reference state (0˚C ice phase).

$$Q_p = P_s C_s \rho_w \min(T_a, 0) + P_r \left[h_f \rho_w + C_w \rho_w \max(T_a, 0) \right] \quad (33)$$

Turbulent fluxes, Q_h, Q_e, E

Sensible and latent heat fluxes between the snow surface and air above are modeled using the concept of flux proportional to temperature and vapor pressure gradients. The constants of proportionality are the so-called turbulent transfer coefficients which are functions of windspeed and surface roughness. Considering a unit volume of air, the heat content is $\rho_a C_p T_a$ and the vapor content $\rho_a q$, where ρ_a is air density (determined from atmospheric pressure and temperature), C_p air specific heat capacity [1.005 kJ kg^{-1} $^oC^{-1}$], and q specific humidity [kg water vapor per kg air]. Heat transport towards the surface, Q_h [$kJ/m^2/hr$] is given by:

$$Q_h = K_h \rho_a C_p \left(T_a - T_s \right) \quad (34)$$

where K_h is heat conductance [m/hr] and T_s is the snow surface temperature. Vapor transport away from the surface (sublimation), M_e [kg/hr] is:

$$M_e = K_e \rho_a (q_s - q) \quad (35)$$

where q_s is the surface specific humidity and K_e the vapor conductance [m/hr].

By comparison with the usual expressions for turbulent transfer in a logarithmic boundary layer profile (*Anderson*, 1976; *Male and Gray*, 1981; *Brutsaert*, 1982) for neutral condition, one obtains the following expression:

$$K_h = K_e = K_{neutral} = \frac{k^2 V}{\left[1n (z/z_o) \right]^2} \quad (36)$$

where V is wind speed [m/hr] at height z [m]; z_o is roughness height at which the logarithmic boundary layer profile predicts zero velocity [m]; and k is von Karman's constant [0.4]. When there is a temperature gradient near the surface, buoyancy effects may enhance or dampen the turbulent transfers. This effect can be quantified in terms of the Richardson number or Monin-Obukhov length. The code we wrote includes adjustments based on the Richardson number.

$$R_i = \frac{(g/T)\, dT/dz}{(dV/dz)^2} \approx \frac{g(T_a - T_s)\, z}{V^2\, T_a} \tag{37}$$

The heat and vapor conductances, K_h and K_e obtained from (36) and used in (34) and (35) are adjusted using the following (*Price and Dunne*, 1976)

$$K_{adj} = K_{neutral}/(1 + 10\, R_i) \quad R_i > 0, \text{ Stable or inversion conditions.} \tag{38}$$

$$K_{adj} = K_{neutral}\,(1 - 10\, R_i) \quad R_i < 0, \text{ Unstable or lapse conditions.} \tag{39}$$

While testing the model we found that it was quite common that large temperature differences and low wind speeds resulted in unreasonable correction factors, beyond the range for which they had been developed, so we included in the code a factor F_{stab} that controls the extent to which these corrections are applied:

$$K_h = K_e = K_{neutral} + F_{stab}(K_{adj} - K_{neutral}) \tag{40}$$

Putting $F_{stab} = 0$ uses neutral conductances. Putting $F_{stab} = 1$ gives the full stability corrections and F_{stab} between 0 and 1 interpolates between these. Currently we recommend using $F_{stab} = 0$, until the question of unreasonable correction factors can be resolved. All the results presented here used $F_{stab} = 0$.

Recognizing that the latent heat flux towards the snow is:

$$Q_e = -h_v\, M_e \tag{41}$$

and using the relationship between specific humidity and vapor pressure and the ideal gas law, one obtains:

$$Q_e = K_e \frac{h_v\, 0.622}{R_d\, T_a} \left(e_a - e_s(T_s)\right) \tag{42}$$

where e_s is the vapor pressure at the snow surface snow, assumed saturated at T_s, and calculated using a polynomial approximation (*Lowe*, 1977); e_a is air vapor pressure, R_d is the dry gas constant [287 J kg^{-1} K^{-1}] and h_v the latent heat of sublimation [2834 kJ/kg]. The water equivalence depth of sublimation is:

$$E = -\frac{Q_e}{\rho_w h_v} \tag{43}$$

Snow Surface Temperature, T_s

Since snow is a relatively good insulator, T_s is in general different from T. This difference is accounted for using an equilibrium approach that balances energy fluxes at the snow surface. Heat conduction into the snow is calculated using the temperature gradient and thermal diffusivity of snow, approximated by:

$$Q = \kappa \rho_s C_s (T_s - T)/Z_e = K_s \rho_s C_s (T_s - T) \tag{44}$$

where κ is snow thermal diffusivity [m^2 hr^{-1}] and Z_e [m] an effective depth over which this thermal gradient acts. The ratio κ/Z_e is denoted by K_s and termed snow surface conductance, analogous to the heat and vapor conductances. A value of K_s is obtained by assuming a depth Z_e equal to the depth of penetration of a diurnal temperature fluctuation calculated from equation (6) (*Rosenberg*, 1974). Z_e should be chosen so that R_z/R_s is small. Here K_s is used as a tuning parameter, with this calculation used to define a reasonable range. Then assuming equilibrium at the surface, the surface energy balance gives:

$$Q = Q_{sn} + Q_{li} + Q_h(T_s) + Q_e(T_s) + Q_p - Q_{le}(T_s) \tag{45}$$

where the dependence of Q_h, Q_e, and Q_{le} on T_s is through equations (34), (42) and (26) respectively.

Analogous to the derivation of the Penman equation for evaporation the functions of T_s in this energy balance equation are linearized about a reference temperature T*, and the equation is solved for T_s:

$$T_s = \frac{Q_{sn} + Q_{li} + Q_p + K T_a \rho_a C_p - 0.622 K h_v \rho_a \left(e_s(T^*) - e_a - T^* \Delta \right)/P_a + 3\varepsilon_s \sigma T^{*4} + \rho_s C_s T K_s}{\rho_s C_s K_s + K \rho_a C_p + 0.622 \Delta K h_v \rho_a / P_a + 4 \varepsilon_s \sigma T^{*3}} \tag{46}$$

where $\Delta = de_s/dT$ and all temperatures are absolute [˚K]. This equation is used in an iterative procedure with an initial estimate $T^* = T_a$, in each iteration replacing T* by the latest T_s. The procedure converges to a final T_s which, if less than freezing, is used to calculate surface energy fluxes. If the final T_s is greater than freezing it means that the energy input to the snow surface cannot be balanced by thermal conduction into the snow. Surface melt will occur and the infiltration of meltwater will account for the energy difference and T_s is then set to 0˚C.

Meltwater Outflux, M_r and Q_m

The energy content state variable U determines the liquid content of the snowpack. This result, together with Darcy's law for flow through porous media, is used to determine the outflow rate.

$$M_r = K_{sat} S^{*3} \tag{47}$$

where K_{sat} is the snow saturated hydraulic conductivity and S* is the relative saturation in excess of water retained by capillary forces. This expression is based on Male and Gray (1981, p. 400, eqn 9.45). S* is given by:

$$S^* = \frac{\text{liquid water volume - capillary retention}}{\text{pore volume - capillary retention}} = \left(\frac{L_f}{1 - L_f} - L_c \right) / \left(\frac{\rho_w}{\rho_s} - \frac{\rho_w}{\rho_i} - L_c \right) \tag{48}$$

where $L_f = U/(\rho_w h_f W)$ denotes the mass fraction of total snowpack (liquid and ice) that is liquid, L_c [0.05] the capillary retention as a fraction of the solid matrix water equivalence, and ρ_i the density of ice [917 kg m^{-3}]. This melt outflow is assumed to be at 0˚C so the heat advected with it, relative to the solid reference state is:

$$Q_m = \rho_w h_f M_r \tag{49}$$

Forest Cover

The presence of vegetation, especially forests, significantly influences energy exchanges at the snow surface. A forest canopy reduces wind speed, thus reducing sensible and latent heat transfers. It also affects the radiation exchanges. The penetration of radiation through vegetation has been widely studied (*Sellers et al.*, 1986; *Verstraete*, 1987a; 1987b; *Verstraete et al.*, 1990; *Dickinson et al.*, 1993), and models have been developed that discretize the canopy into layers treating the energy balance of each layer separately (*Bonan*, 1991). Here we avoid these complexities and adopt a pragmatic parameterization modeled after the representation of snowmelt used by the WEPP winter routines (*Hendrick et al.*, 1971; *Young et al.*, 1989). Forest cover is parameterized by the canopy density parameter F_c, representing the canopy closure fraction (between 0 and 1). Windspeed, and therefore the corresponding heat and vapor fluxes, are reduced by a factor ($1-0.8F_c$). Radiative fluxes Q_{sn}, Q_{li} and Q_{le} in equation (1) are reduced by a factor ($1-F_c$). Adjustments are also made to the radiation terms in the calculation of snow surface temperature (equation 43).

Calibration And Testing

It was a design goal that this model be physically based without requiring calibration at different locations. We believe the model goes a long way towards achieving this goal. However in its development some parameters requiring parameterization were introduced. The approach taken was to calibrate these parameters with data from the Central Sierra Snow Laboratory for the winter of 1985-1986. These parameters are intended to be transportable and we test the model using these same parameters against data from the Reynolds Creek Experimental Watershed, Boise, Idaho and USU drainage and evapotranspiration research farm, Logan Utah. An independent test was conducted by Robert Harrington at the University of Arizona using data from Mamoth mountain. These results are also presented.

Central Sierra Snow Laboratory - Calibration

The CSSL located 1 km east of Soda Springs, California, measures and archives comprehensive data relevant to snow. It is at latitude 39˚19'N and at elevation 2100 m. The meteorological data is reported each hour and consists of temperature, radiation, humidity, precipitation, and wind measurements at two levels in a 40 x 50 m clearing and in a mixed conifer fir forest with 95% forest cover. Only data from the clearing are used here. Snow depths and water equivalence are measured daily (except on weekends) and eight lysimeters record melt outflow each hour. We used the temperature, precipitation, radiation (incoming solar and net), humidity and wind measurements to drive our model and compared model output to measurements of snow water equivalence, melt outflow and snow surface temperature (infrared sensor).

The model was calibrated against the CSSL data for the winter 1985 - 1986. The energy balance and overall accumulation and ablation of the snowpack is governed primarily by surface energy exchange processes. The adjustable parameters involved in these are z_o and K_s, which were adjusted to obtain a match between modeled and observed water equivalence (shown in Fig. 4), and modeled and observed snow surface temperatures (Fig. 5), with the model driven by the measured net radiation input. We then used measured incoming solar radiation to drive the model and found that the melt is delayed (Fig. 4). Discrepancies were analyzed and attributed to differences in daytime net radiation, primarily affected by albedo. The albedo parameterization (*Dickinson et al.*, 1993) has parameters $\alpha_{vo} = 0.95$ and $\alpha_{nir} = 0.65$ which represent the reflectance of new snow in the visible and infrared ranges. α_{vo} was reduced to 0.85 to match the daytime net radiation when compared to measured CSSL 1985 - 1986 data (Fig. 6). The resulting snow water equivalence comparison (Fig. 4) indicates that some early season melt is not modeled resulting in slight over accumulation, but the main melt is well modeled. In all results except the line indicated on Fig. 4, $\alpha_{vo} = 0.85$ was used. Melt outflow rate was compared to the average

from the eight melt lysimeters, with K_{sat} adjusted to get a good fit. Results are shown in Fig. 7.

Table 1 lists the adjustable parameters that were calibrated against the CSSL data. Table 2 lists the remaining model parameters which were held fixed at their nominal values.

Table 1. Adjustable parameter recommended values.

Parameter	Notation	Calibrated Value
Surface aerodynamic roughness	z_o	0.005 m
Surface heat conductance	K_s	0.02 m/hr
Saturated hydraulic conductivity	K_{sat}	20 m/hr
New snow visible band reflectance	α_{vo}	0.85

Table 2. Snowmelt model fixed parameters.

Parameter	Notation	Reference Value
Ground heat capacity	C_g	2.09 kJ kg^{-1} $^{\circ}C^{-1}$
Density of soil layer	ρ_g	1700 kg m^{-3}
Snow density	ρ_s	450 kg m^{-3}
Capillary retention fraction	Lc	0.05
Emissivity of snow	ε_s	0.99
Temperature above which precipitation is rain	T_r	3˚C
Temperature below which precipitation is snow	T_s	-1˚C
Wind/air temperature measurement height	z	2 m
Soil effective depth	D_e	0.4 m
Bare ground albedo	A_{bg}	0.25
New snow near infrared band reflectance	α_{iro}	0.65

These parameter values are recommended for application of the model without additional calibration. In the tests below (except Mamoth mountan) these parameters were used.

Reynolds Creek Experimental Watershed - Testing

Upper Sheep Creek is a 26 ha catchment within the semi-arid Reynolds Creek experimental watershed. Snowmelt is the main hydrologic input and its areal distribution is heavily influenced

by wind induced drifting. Detailed descriptions of the various features of the area are given in Flerchinger et al. (1992) and references therein. Snow water equivalence measurements are made biweekly (as weather permits) on a 30.48 m (100 ft) grid over the watershed. A digital elevation model (DEM) was constructed from a 1:1200 map with 0.61 m (2 ft) contour interval developed from low-level aerial photography. The DEM grid was constructed to coincide with the grid used for field measurements and provided slope and aspect inputs to the model radiation calculations. Figure 8 shows the topography and grid over Upper Sheep Creek together with locations of some of the instrumentation. Data from the winters of 1985 - 1986 and 1992 - 1993 were used in this study to test the model running in a distributed mode at each grid cell. Snowmelt outputs were used as hydrologic inputs for a water balance study (*Jackson*, 1994; *Tarboton et al.*, 1995).

The model was tested against the data from Reynolds Creek and USU drainage and evapotranspiration research farm without further adjustment of parameters. The Reynolds Creek study applied the model to each 30.48 x 30.48 m grid cell over Upper Sheep Creek (Fig. 8). The drift factor to adjust snow input was estimated from the observed gridded snow data for 1985-1986 (*Jackson*, 1994; *Jackson et al.*, 1996). Fig. 9 shows the drift factors and Fig. 10 compares measured and modeled spatial distribution of snow on three dates during the snowmelt phase in 1992-1993. These results indicate that the model correctly represents the spatial accumulation and melt patterns. Figure 11 shows simulated and observed snowmelt as recorded at two melt collectors in Upper Sheep Creek. These indicate some discrepancies in the simulation of melt from the snow drift located at L10. Figure 12 shows modeled and observed area average snow water equivalence at Upper Sheep Creek for the two years 1985/6 and 1992/3. In 1992/3 the drift accumulations appeared to be less than 1985/6. Since the drift factors were calibrated from 1985/6 there is an over prediction in 1992/3. However when the model is initialized on 3/3/93 with observed snow amounts and little additional accumulation the reproduction of overall ablation is good.

USU drainage and evapotranspiration research farm - testing

An experiment to measure snow energy balance and sublimation from snow in the winter of 1992 - 1993 is described more fully by Tarboton (1994). The USU drainage and evapotranspiration experimental farm is located in Cache Valley near Logan, Utah, USA (41.6˚ N, 111.6˚ W, 1350 m elevation). The weather station and instrumentation are in a small fenced enclosure at the center of a large open field. There are no obstructions to wind in any direction for at least 500 m. Cache Valley is a flat bottomed valley surrounded by mountains that reach elevations of 3000 m. During the period of this experiment the ground was snow covered from November 20, 1992 to March 22, 1993. Air temperatures ranged from -23 ˚C to 16 ˚C and there was 190 mm of precipitation (mostly snow, but some rain). The snow accumulated to a maximum depth of 0.5 m with maximum water equivalence of 0.14 m. Data collected included measurements of snow water equivalence, snow surface temperature and the meteorological variables necessary to drive our

model. Temperatures within the snow were measured using a ladder of thermocouples suspended on fishing line strung between two upright posts at 75 mm spacing. The instrumentation also included two weighing lysimeters comprising 1 x 1 x 1 m metal boxes embedded flush with the surface and filled with soil, vegetated with grass similar to the surrounding agricultural field. Load cells (underneath in the case of one lysimeter and at the corners for the other) record the weight of soil, grass, soil moisture and snow over the 1 m^2 areas. Meltwater infiltrates into the lysimeter and so does not result in a weight change. Changes in weight are due only to addition or removal of mass from the surface, which in the case of snow can be due to precipitation, condensation, sublimation and wind drifting.

Figure 13 gives the measured lysimeter weights, snow water equivalences and accumulated precipitation. The measured snow water equivalence values shown are the average from 8 snow core measurements made each visit. The individual water equivalence measurements usually varied within a range of 10 to 20% from this average. This shows general agreement between weight accumulation on the lysimeters, snow accumulation, and precipitation. Figure 14 compares modeled and measured snow water equivalence for the model run from day 26 to the end of the melt period. Two model runs are shown, one with the model driven by measured net radiation and the other with the model driven by incoming solar radiation. The first run bypasses the albedo and outgoing longwave radiation calculations so serves only to test the model's sensible and latent heat flux components. The second run is a more realistic check on overall model performance. For both runs the model was initialized with the measured day 26 water equivalence of 0.104 m and energy content based on the average temperature of thermocouples in the snow and soil. This energy content was -1136 kJ/m^2. These results show that the model does reasonably well at representing snow accumulation and melt. The second model run, with solar radiation as the primary energy input, was used for the remainder of the comparisons.

Figure 15 shows modeled and measured snow (and soil) energy content. The measured energy content was estimated from the measured water equivalence (linearly interpolated between measurements) and snow and soil temperatures averaged from the thermocouple ladder measurements. There is obviously a large discrepancy between modeled and measured energy content early on, and given this it is surprising how well the model does at representing other aspects of the snow accumulation and melt processes. The lowest energy content on day 39 would predict an average snow and soil temperature of -14 ˚C. This is well below the observed snow temperatures shown on figure 16. These discrepancies indicate that the model overestimates the loss of energy during cold periods, suggesting that the snow surface conductance may be too large. It also indicates that temperature fluctuations do not penetrate to the full interacting soil layer depth, D_e [0.4 m] suggesting that perhaps D_e should be reduced. There may also be a problem with ground heat flux which was input as zero in these runs, but may not be. After day 70 (March 20) the model energy content is above zero due to the liquid water content of the snow. This is the

melt period. The measured energy, estimated from thermocouple measurements of snow and soil temperatures, does not account for liquid water in the snow.

Figure 17 compares modeled and measured infrared snow surface temperatures during portion of the premelt period. This indicates that the equilibrium procedure for calculation of snow surface temperature works reasonably well. Detailed results for the melt period (March 19, day 69 to March 23, day 82) are shown in figures 18a-h. The onset of melt was triggered by the 20 mm of precipitation, falling as a mixture of rain and snow, on days 69 and 70. Following the precipitation strong winds and low humidity (vapor pressure, figure 18g) induces sublimation in the model over days 71 and 72 (figure 18h). There is some suggestion of a downward trend (implying sublimation) in the lysimeter trace on figure 18a. With this sublimation and cooler air temperatures there is minimal melt modeled on days 71 and 72. Freezing of the snow surface is well modeled as indicated by the model and measured snow surface temperatures (figure 18f). Warmer weather and higher humidity beginning on day 73 are characterized by positive sensible heat (higher temperatures at the upper sensor, fig 18e) and condensation (higher vapor pressure at the higher sensor, fig 18g) which both add energy to the snowpack, which consequently melts rapidly. The horizontal dashed line on figure 18g is 6.1 mb, the saturation vapor pressure of water over ice at freezing point. Vapor pressures higher than this imply a downward vapor pressure gradient which will result in condensation. Rain on day 76 makes melting even more rapid. Figure 18a indicates that over the whole season, according to the model, net sublimation was only a small fraction (the difference between the dashed lines) of the snow mass. This was due to the persistent inversions and high humidity associated with valley fog.

Mammoth Mountain - testing

Robert Harrington at the University of Arizona conducted an evaluation of two snowmelt models (SNTHRM) (*Jordan,* 1991), and the UEB model described here (*Harrington et al.,* 1995). In what follows I summarize some of his results which represent an independent test of UEB. Harrington did not use the recommended parameters listed in tables 1 and 2 above. Instead he calibrated parameters to achieve complete ablation approximately when it was observed to occur in the field. The parameter values calibrated, different from the recommended values in tables 1 and 2 were:

Surface aerodynamic roughness	z_o	0.00001 m
Surface heat conductance	K_s	0.2 m/hr
New snow visible band reflectance	α_{vo}	1.0
New snow near infrared band reflectance	α_{iro}	0.8
Bare ground albedo	A_{bg}	0.3
Liquid holding capacity	L_c	0.04

Soil effective depth	D_e	0.2 m

The model is quite sensitive to the first four of these variables and relatively insensitive to the last three. The model was driven by measured incident solar radiation.

The field data set used was from Mammoth Mountain, California, for the time period April to July 1993. This data consists of time series of snow water equivalence measured in pairs of biweekly snow pits, lysimeter discharge from seven 1x1 m lysimeters at the base of the snow pack measured semihourly and meteorological variables recorded at fifteen minute intervals. The site is at 2895 m above sea level on a sparsely timbered subalpine knoll within the boundaries of the Mammoth Mountain Ski Area. The lysimeters are arranged in two clusters on the north and south side of the meteorological instrument tower.

The model results are compared on the basis of snow water equivalence, meltwater efflux, measured from the lysimeters in each cluster, and albedo. Measured meltwater efflux from the lysimeters was found to be very variable so to impose a degree of mass balance self consistency on the data lysimeter melt outflow was scaled so that the cumulative efflux corresponded to observed initial snow water equivalence plus subsequent precipitation. Figure 19 compares observed and modeled snow water equivalence (SWE) at Mammoth Mountain. Figures 20 and 21 compare observed and modeled meltwater efflux. Figure 22 compares modeled and measured albedo. These results show that the UEB model performs adequately at representing the overall ablation of the snowpack at Mammoth. In terms of meltwater efflux the UEB model captures the early season onset of melt efflux nicely and also provides a reasonable estimate for peak daily efflux rates. There are some problems in representing the timing of daily melt pulses when the snowpack is deep. These are evident around day 140 for the south lysimeter cluster. The lag time for penetration of a wetting front generated by energy inputs at the surface of a deep snowpack is evidently not well represented by the melt outflow parameterization used. The modeled albedo is on average somewhat more than measured. Some of this difference may have been due to use of the value 0.95 for new snow visible albedo parameter α_{vo} in place of the recommended 0.85.

Conclusions

This report has provided a detailed description of the scientific approach and mathematical parameterizations used in the UEB snowmelt model. It has also summarized the tests of the model against a range of data. These tests indicate that the lumped (single layer) model that represents the snowpack in terms of two primary state variables performs adequately in terms of predicting snowmelt in open conditions. It still remains essentially untested under forested conditions where sufficient data to test the model has so far not been available. The model has deficiencies that show up when comparing measured and modeled energy content and deficiencies in the

parameterizations of turbulent fluxes, expecially with respect to atmospheric stability/instability. The parameterization of melt outflow does not capture well the timing of diurnal melt under deep snwopacks. Future work should focus on these deficiencies.

II. GUIDE TO USING THE MODEL (UEB)

UEB was developed on a UNIX system using standard fortran 77. It has also been run under DOS and should be portable to any fortran 77 environment. The source code is contained in three files:

snowd.f Primary driving program

snowdgt.f Main snow subroutine and associated subroutines and functions

snowx.f Auxiliary subroutines used by snowd.f, but not snowdgt.f. Most of these are for radiation and time calculations.

The distribution also includes a separate program **trange.f** that can be used to calculate monthly average diurnal temperature ranges used with the Bristow and Campbell (1984) procedure for estimating incoming solar radiation from diurnal temperature ranges.

The core of the model is the subroutine named SNOW and the functions and subroutines it calls. These are all in file snowdgt.f. The subroutine SNOW is intended to provide a snow model component that can be linked with other programs such as WEPP, or a spatially distributed model (e.g. *Jackson*, 1994; *Jackson et al.*, 1996) that comprise a more complete modeling system. In order to provide stand alone capability the file **snowd.f** contains is a simple program (referred to as SNOWD) to process input and output and drive the SNOW subroutine. The SNOW subroutine requires as input solar and longwave radiation as well as air temperature, precipitation, wind speed, relative humidity and solar illumination angle cosine. In cases where the radiation is not available the main program provides estimates using the methodology described above. The subroutines and functions used to make these estimates are in file snowx.f.

Using the model with driving program SNOWD.

Model input is from four files:

1. Weather file
2. Model parameter file
3. Site variable file
4. Bristow Campbell parameter file

The output is also written to a file. The program prompts for and the user is required to input names for these files. The program also prompts for the type of radiation input being used and the user is required to enter 0, 1 or 2 designating one of the following choices:

0. Incoming solar radiation is to be estimated from daily temperature range.
1. Measured incoming solar radiation.
2. Measured Net radiation.

The users response is designated IRADFL and its the value dictates the radiation input format as specified below.

Following are format specifications and examples of these files.

Weather file

The first record contains: Start month, start day, start year, start hour, time step (hours), initial energy
content U (kJ/m^2), Initial water equivalence W (m), Initial snow surface age.

The second record contains the number of input lines to skip if you want to jump ahead in the input file. Usually it is 0.

The remaining records contain in free format 7 columns of input data as follows:

1. Air Temperature (in ˚C).
2. Precipitation rate (in m/hr).
3. Wind Speed (in m/s).
4. Relative humidity (as a fraction).
5. Daily air temperature range (max - min). This is used to infer solar radiation input if this is not given, and to infer cloudiness for the longwave radiation input. This is only used if IRADFL = 0.
6. Incoming shortwave. Only used if IRADFL=1.
7. Net radiation. Only used if IRADFL = 2.

Example

```
5 16 86 0. 6. 21852.20 1.240756 0.56845
0
6.506857 0.000000 1.828394 0.500000 9.600000 0.000000 475.250000
11.290192 0.000000 2.304491 0.435833 9.600000 1585.991455 475.500000
15.373524 0.000000 2.724709 0.353000 9.600000 1489.272705 475.750000
12.223524 0.000000 1.113130 0.321000 9.600000 0.000000 476.000000
12.023525 0.000000 2.205397 0.405500 7.700000 0.000000 476.250000
...  etc.
```

Model parameter file: Suggested name **param.dat**

This file is free format containing model parameters in the following order.

1. T_r Temperature above which all precipitation is rain (3 ˚C).
2. T_s Temperature below which all precipitation is snow (-1 ˚C).
3. T_o Temperature of freezing (0 ˚C).
4. TK Constant to convert ˚C to Kelvin (273.15).
5. ε_s emissivity of snow (nominally 0.99).

6. σ Stefan boltzman constant (2.0747e-7 kJ/m^2/hr/K).
7. h_f Heat of fusion (333.5 kJ/kg).
8. h_v Heat of Vaporization (Ice to Vapor, 2834 kJ/kg).
9. C_w Water Heat Capacity (4.18 kJ/kg/C).
10. C_s Ice heat capacity (2.09 kJ/kg/C).
11. C_g Ground heat capacity (nominally 2.09 kJ/kg/C).
12. C_p Air Heat Capacity (1.005 kJ/kg/K).
13. R_d Ideal Gas constant for dry air (287 J/kg/K).
14. k Von Karman's constant (0.4).
15. z Nominal measurement height for air temperature and humidity (2 m).
16. z_o Surface aerodynamic roughness (m).
17. HFF Factor to convert hours into seconds (3600).
18. ρ_i Density of Ice (917 kg/m^3).
19. ρ_w Density of Water (1000 kg/m^3).
20. ρ_s Snow Density (nominally 450 kg/m^3).
21. ρ_g Soil Density (nominally 1700 kg/m^3).
22. L_c Liquid holding capacity of snow (0.05).
23. K_{sat} Snow Saturated hydraulic conductivity (20 m/hr).
24. D_e Thermally active depth of soil (0.4 m).
25. K_s Snow Surface thermal conductance (m/hr).
26. g Gravitational acceleration (9.81 m/s^2).
27. A_{bg} Bare ground albedo (0.25).
28. α_{vo} New snow visible band reflectance (0.85).
29. α_{iro} New snow near infrared band reflectance (0.65).
30. F_{stab} Stability correction control parameter (0).

In keeping with the idea that the model is transportable these same parameters should be used in all applications of the model.

Example **param.dat.**

```
3  -1  0  273.15  0.99  2.0747e-7
333.5 2834 4.18 2.09 2.09 1.005
287 0.4 2 0.005 3600
917 1000 450 1700
0.05 20 0.4 0.02 9.81 0.25 0.85 0.65
0
```

Site variable file

Row 1:

1. Forest cover fraction (a number between 0 and 1)
2. Drift factor (a number that precipitation in the form of snow is multiplied by to account for drift accumulations)
3. Atmospheric pressure (Pa)
4. Ground heat flux [kJ/m^2/hr]
5. Albedo extinction depth [m] When snow depth is shallower than this albedo is interpolated between snow value and bare ground value. This should reflect the ground roughness or shrub height.

Row 2:

1. Slope (in degrees)
2. Aspect (in degrees clockwise from north)
3. Latitude (in degrees)

Example site variable file

```
0.0  1.0 88500   0 0.1     fc  df   pr(Pa)  qg aep
0     125.0  39.32    slope aspect lat
```

The text following the numbers in not required. It is simply there as an aid when editing the file.

Bristow Campbell parameter file

Row 1: Parameters a (=0.8) and c (=2.4). 0.8 and 2.4 are values Bristow and Campbell arrived at.

Remaining rows:

Column 1. month

Column 2. Climate average monthly diurnal temperature range (˚C).

Column 3. Number of days that average is based on. This is retained for information only.

Example Bristow Campbell parameter file

```
 0.8  2.4    A, C
 11   10.31950              30
 12   10.17097              31
 1   8.388709              31
 2   7.116965              28
 3   9.766936              31
 4   9.982500              30
 5   13.22661              31
```

There needs to be an entry in this file for each month for which the model will be run.

Ideally this data should be obtained from a long weather station record. In many cases this information is unavailable or hard to obtain so the program **trange** has been provided to compute these statistics from data in the format required for input to the snowmelt model. **trange** is compiled using:

```
f77 trange.f -o trange
```

or the equivalent on a non unix system. It is then run using

```
trange < preweatherfile >weatherfile
```

The `preweatherfile` must be in the same format as the `weatherfile` described above, except that column 5 should contain dummy information (e.g. 0's). `trange` will based on the temperature data in column 1 compute the diurnal temperature range and put it in column 5 in the output `weatherfile`. `trange` will also create an output file `trange.out` that contains the monthly averages based on the data in `weatherfile` that can be used in the Bristow-Campbell file. `trange` computes daily temperature range as daily maximum minus the average of that says and the subsequent days minimum temperatures.

Output file

Free format as follows:

1. Year
2. Month
3. Day
4. Hour
5. Atmospheric transmission factor Tf calculated from Bristow Campbell procedure.
6. Hourly radiation index HRI. Integration of zenith angle cosine over time step. When radiation data is not input, IRADFL set to 0, incoming solar radiation is calculated as Tf * HRI * Solar constant.
7. Air temperature (˚C) repeated from input.
8. Precipitation rate [m/hr] from input.
9. Wind Speed [m/s] from input.
10. Relative humidity fraction from input.
11. Incoming solar radiation ($kJ/m^2/hr$) from input if IRADFL = 1, computed if IRADFL = 0, not used if IRADFL = 2.
12. Incoming longwave radiation ($kJ/m^2/hr$) computed from air temperature and humidity using Satterlund Formula.
13. Zenith angle cosine.
14. Snow energy content state variable [kJ/m^2].

15. Snow water equivalence state variable [m].
16. Snow albedo state variable. This is used differently depending on how albedo is calculated. The code snowd.f is fixed to set iflag(4) to 1 which tells the subroutine snowdgt.f to use the BATS albedo routines. In this case this quantity is the dimensionless snow surface age. Setting iflag(4) to 0 permits the albedo to be input, in which case this is the input value.
17. Part of precipitation that is rain [m/hr].
18. Part of precipitation that is snow [m/hr].
19. Albedo.
20. Sensible heat flux [kJ/m^2/hr].
21. Latent heat flux [kJ/m^2/hr].
22. Sublimation [m].
23. Melt outflow rate [m/hr].
24. Energy advected with melt [kJ/m^2/hr].
25. Sum of energy fluxes into/out of snow [kJ/m^2/hr].
26. Sum of mass fluxes into/out of snow [m/hr].
27. Snow average temperature [˚C].
28. Snow surface skin temperature [˚C].
29. Cumulative precipitation from beginning of model run [m].
30. Cumulative sublimation from beginning of model run [m].
31. Cumulative melt outflow from beginning of model run [m].
32. Net radiation [kJ/m^2/hr],
33. Mass balance error [m]. Should always be close to zero. It reflects computation and rounding errors in the model calculations.

Free format output of all data is used to facilitate input of this into graphics programs for post processing analysis.

Example output file

```
86  5  16    6.00000   0.699027    7.34508E-02    6.50686  0.    1.82839
 0.500000  0.    1012.70    6.91051E-02
  21823.4    1.24058   0.615088  0.  0.   0.752040    198.774   -75.2959
  2.65688E-05    2.95629E-06   0.985922   -4.80559   -2.94711E-05  0.  -0.203033
0.    1.59413E-04    1.77377E-05   -127.298
0.
86  5  16    12.0000   0.699027   0.722090    11.2902  0.    2.30449   0.435833
  1585.99    1097.51   0.679367
  27041.2    1.24013   0.664768  0.  0.   0.655742    414.463   -22.4281
  7.91392E-06    6.74572E-05    22.4970    869.641   -1.39926E-04  0.  0.  0.
  2.06896E-04    4.22481E-04    500.103
0.
```

```
  86  5  16    18.0000   0.699027   0.509350    15.3735  0.    2.72471   0.353000
    1489.27    1167.46   0.479215
    33149.5    1.23680   0.714448  0.  0.   0.653158    657.828    4.92099
   -1.73641E-06    5.55642E-04    185.307    1018.05   -9.83952E-04  0.  0.  0.
    1.96478E-04    3.75633E-03    540.608
    1.19209E-07
  86  5  17  0.   0.699027    9.67353E-03    12.2235  0.    1.11313   0.321000
  0.    1096.32    9.10120E-03
    32307.4    1.23218   0.764128  0.  0.   0.780674    216.037   -59.3330
    2.09361E-05    7.49567E-04    249.981   -140.344   -6.94039E-04  0.  0.  0.
    3.22094E-04    8.25374E-03   -47.0675
    1.19209E-07
  86  5  17    6.00000   0.563609    7.49376E-02    12.0235  0.    2.20540
   0.405500  0.    1158.86    7.05039E-02
    33128.4    1.22729   0.813808  0.  0.   0.738531    421.317   -31.7891
    1.12170E-05    8.04114E-04    268.172    136.826   -9.22705E-04  0.  0.  0.
    3.89397E-04    1.30784E-02    15.4695
    1.19209E-07
... etc
```

Using the model as a subroutine

The subroutine should be called with a fortran statement like:

```
      call snow(dt,nt,input,sitev,statev,param,iflag,
     &                cump,cume,cummr,outv)
```

Table of argument specifications

Name	Type	Input/Output	Description
dt	real	input	Time step (hours)
nt	integer	input	Number of time steps subroutine should execute before returning.
input	real(7,nt)	input	An array of the 7 input variables for each of nt time steps. See note 1.
sitev	real(5)	input	An array of the five site variables from row 1 of the site variable file described above.
statev	real(3)	input and output	State variables U, W and τ. These must be input as

			their initial values and will be returned as the ending value after nt time steps.
param	real(30)	input	An array of the 30 parameters from parameter file described above.
iflag	integer(3)	input	An array of control flags. See note 2.
cump	real	input and output	Cumulative precipitation in m. The program increments this by the precipitation quantity falling during nt time steps.
cume	real	input and output	Cumulative sublimation in m. The program increments this by the sublimation quantity falling during nt time steps.
cummr	real	input and output	Cumulative melt runoff in m. The program increments this by the quantity of melt runoff generated during nt time steps.
outv	real(13)	output	Diagnostic variables output from the last time step. See note 3.

Notes.

1. The seven input variables are (in order):
    1. Air Temperature (˚C);
    2. Precipitation rate (m/hr);
    3. Wind Speed (m/s);
    4. Relative humidity fraction

    If INETR = 0

        5. Incoming shortwave radiation ($kJ/m^2/hr$)
        6. Incoming longwave radiation ($kJ/m^2/hr$)

    If INETR = 1

        5. Incoming net radiation ($kJ/m^2/hr$)
        6. Unused

    7. Representative cosine of illumination angle for use in albedo calculation.
2. The three control flags are
    1. INETR. Used to designate whether input is short and longwave radiation or net radiation.
    2. PFLAG. Used to designate whether output is to be written to file at each time step. Values: 1 Write output; anything else no output.
    3. OUNIT. Fortran unit number for writing of output if designated by PFLAG.
3. If PFLAG= 1 the following variables are written in free format to unit number OUNIT.
    1. Rainfall (m/hr). Part of precipitation modeled as rain.
    2. Snowfall (m/hr). Part of precipitation modeled as snow.

3. Albedo.
4. Sensible heat flux Q_h (kJ/m^2/hr).
5. Latent Heat flux Q_e (kJ/m^2/hr).
6. Sublimation (m/hr).
7. Melt outflow rate (m/hr).
8. Heat advected by melt outflow Q_m (kJ/m^2/hr).
9. Total surface energy flux into the snow Q (kJ/m^2/hr).
10. Combined mass fluxes (dW/dt) (m/hr).
11. Snow and underlying soil average temperature T (˚C).
12. Snow surface temperature, T_S (˚C).
13. Net radiation (kJ/m^2/hr).

References

Anderson, E. A., (1968), "Development and Testing of Snow Pack Energy balance equations," Water Resources Research, 4(1): 19-37.

Anderson, E. A., (1973), "National Weather Service River Forecast System-Snow Accumulation and Ablation Model," NOAA Technical Memorandum NWS HYDRO-17, U.S. Dept of Commerce.

Anderson, E. A., (1976), "A Point Energy and Mass Balance Model of a Snow Cover," NOAA Technical report NWS 19, U.S. Department of Commerce.

Anderson, E. A. and N. H. Crawford, (1964), "The synthesis of continuous snowmelt hydrographs on a digital computer," Technical Report no 36, Stanford University Department of Civil Engineering.

Bonan, G. B., (1991), "A Biophysical Surface Energy Budget Analysis of Soil Temperature in the Boreal Forests of Interior Alaska," Water Resources Research, 27(5): 767-781.

Bras, R. L., (1990), Hydrology, An introduction to hydrologic science, Addison-Wesley, Reading, MA, 643 p.

Bristow, K. L. and G. S. Campbell, (1984), "On the Relationship Between Incoming Solar Radiation and the Daily Maximum and Minimum Temperature," Agricultural and Forest Meteorology, 31: 159-166.

Brunt, D., (1952), Physical and Dynamical Meteorology, Cambridge University Press, Cambridge.

Brutsaert, W., (1975), "On a deriveable formula for long-wave radiation from clear skies," Water Resources Research, 11: 742-744.

Brutsaert, W., (1982), Evaporation into the Atmosphere, Kluwer Academic Publishers, 299 p.

Charbonneau, R., J. P. Lardeau and O. C, (1981), "Problems of modelling a high mountainous drainage basin with predominant snow yields," Hydrological Sciences Bulletin, 26(4): 345-361.

Colbeck, S. C., (1978), "The physical aspects of water flow through snow," Advances in Hydroscience, 11.

Colbeck, S. C., (1991), "The layered character of snow covers," Reviews of Geophysics, 29(1): 81-96.

Dickinson, R. E., A. Henderson-Sellers and P. J. Kennedy, (1993), "Biosphere-Atmosphere Transfer Scheme (BATS) Version 1e as Coupled to the NCAR Community Climate Model," NCAR/TN-387+STR, National Center for Atmospheric Research.

Dingman, S. L., (1994), Physical Hydrology, Macmillan, 575 p.

Dozier, J., (1979),"A Solar Radiation Model for a Snow Surface in Mountainous Terrain," in Proceedings Modeling Snow Cover Runoff, ed. S. C. Colbeck and M. Ray, U.S. Army Cold Reg. Res. Eng. Lab., Hanover, NH, p.144-153.

Dozier, J., (1987), "Recent research in Snow Hydrology," Reviews of Geophysics, 25(2): 153-161.

Dozier, J. and J. Frew, (1990), "Rapid Calculation of Terrain Parameters for Radiation Modeling From Digital Elevation Data," IEEE Transactions on Geoscience and Remote Sensing, 28(5): 963-969.

Dubayah, R., J. Dozier and F. W. Davis, (1990), "Topographic Distribution of Clear-Sky Radiation Over the Konza Prairie, Kansas," Water Resources Research, 26(4): 679-690.

Flerchinger, G. N., K. R. Cooley and D. R. Ralston, (1992), "Groundwater Response to Snowmelt in a Mountainous Watershed," Journal of Hydrology, 133: 293-311.

Frew, J. E., (1990), "The Image Processing Workbench," PhD Thesis, Geography, University of California, Santa Barbara.

Gary, H. L. and C. A. Troendle, (1982), "Snow Accumulation and Melt Under Various Stand Densities in Lodgepole Pine in Wyoming and Colorado," Research Note RM-417, USDA Forest Service.

Gerald, C. F., (1978), Applied Numerical Analysis, 2nd Edition, Addison Wesley, Reading, Massachusetts, 518 p.

Gray, D. M. and D. H. Male, ed. (1981), Handbook of Snow, Principles, processes, management & use, Pergamon Press, 776 p.

Harrington, R., R. Jordan and D. G. Tarboton, (1995), "A comparison of two energy balance snowmelt models," Eos Trans. AGU, 76(46): Fall Meeting Suppl., F185, Presentation at AGU fall meeting.

Hendrick, R. L., B. D. Filgate and W. M. Adams, (1971), "Application of Environmental Analysis to Watershed Snowmelt," Journal of Applied Meteorology, (10): 418-429.

Jackson, T. H., D. G. Tarboton and K. R. Cooley, (1996), "A Spatially-Distributed Hydrologic Model for a Small Arid Mountain Watershed," Submitted to Journal of Hydrology, UWRL working paper WP-96-HWR-DGT/002.

Jackson, T. H. R., (1994), "A Spatially Distributed Snowmelt-Driven Hydrologic Model applied to the Upper Sheep Creek Watershed," Ph.D Thesis, Civil and Environmental Engineering, Utah State University.

Jordan, R., (1991), "A one-dimensional temperature model for a snow cover," Technical documentation for SNTHERM.89, special technical report 91-16, US Army CRREL.

Kondo, J. and T. Yamazaki, (1990), "A prediction model for snowmelt, snow surface temperature and freezing depth using a heat balance method," Journal of applied meteorology, 29: 375-384.

Kuz'min, P. P., (1961), Protsess Tayaniya Shezhnogo Pokrova (Melting of Snow Cover), [English translation by Israel Prog. Sci. Transl., Transl. 71].

Lane, L. J. and M. A. Nearing, (1989), "USDA-Water Erosion Prediction Project: Hillslope profile model documentation," NSERL Report No. 2, USDA-ARS National Soil Erosion Research Laboratory, West Lafayette, Indiana.

Leavesley, G. H., R. W. Lichty, B. M. Troutman and L. G. Saindon, (1983), "Precipitation-runoff modeling system--Users manual:," Water resources Investigations Report 83-4238, U.S. Geological Survey.

Leavesley, G. H., A. M. Lumb and L. G. Saindon, (1987),"A microcomputer-based watershed-modeling and data-management system," in 55th Annual meeting, Western Snow Conference, April 14-17, p.108-117.

Leu, C. H., (1988), "Evaluation of Spatially-Distributed snowpack estimation using pattern recognition," PhD Thesis, Civil and environmental engineering, Utah State University.

Linsley, R. K., M. A. Kohler and J. L. H. Paulhus, (1975), Hydrology for Engineers, 2nd Edition, McGraw-Hill, Kogakusha, Ltd, 482 p.

Lowe, P. R., (1977), "An Approximating Polynomial for the Computation of Saturation Vapour Pressure," Journal of Applied Meteorology, 16: 100-103.

Male, D. H. and D. M. Gray, (1981), "Snowcover Ablation and Runoff," Chapter 9 in Handbook of Snow, Principles, Processes, Management and Use, Edited by D. M. Gray and D. H. Male, Pergammon Press, p.360-436.

Marks, D. and J. Dozier, (1979), "A Clear-Sky Longwave Radiation Model for Remote Alpine Areas," Archev Fur Meteorologie Geophysik und Bioklimatologie, Ser B, 27: 159-187.

Marshall, S. E. and S. G. Warren, (1987),"Parameterization of snow albedo for climate models," in Large Scale Effects of Seasonal Snowcover, Proceedings of the Vancouver Symposium, August 1987, IAHS Publ. no. 166.

McKay, G. A. and D. M. Gray, (1981), "The distribution of snowcover," in Handbook of Snow, Principles, processes, management & use, Edited by D. M. Gray and D. H. Male, Pergammon press, p.Chapter 5.

Morris, E. M., (1982),"Sensitivity of the European Hydrological System snow models," in Hydrological Aspects of Alpine and High Mountain Areas, Proceedings of the Exeter Symposium, IAHS Publ no 138, p.221-231.

Price, A. G. and T. Dunne, (1976), "Energy balance computations of snowmelt in a subarctic area," Water Resources Research, 12(4): 686-694.

Riley, J. P., D. G. Chadwick and J. M. Bagley, (1966), "Application of electronic analog computer to solution of hydrologic and river basin planning problems: Utah simulation model II," PRWG32-1, Utah Water research lab., Utah State University.

Rosenberg, N. J., (1974), Microclimate The Biological Environment, John Wiley & Sons, Inc., 315 p.

Satterlund, D. R., (1979), "An Improved Equation for Estimating Long-wave Radiation From the Atmosphere," Water Resources Research, 15: 1643-1650.

Sellers, P. J., Y. Mintz, Y. C. Sud and A. Dalcher, (1986), "A simple biosphere model (SiB) for

use with general circulation models," Journal of the Atmospheric Sciences, 43(6): 505-531.

Tarboton, D. G., (1994),"Measurement and Modeling of Snow Energy Balance and Sublimation From Snow," in Proceedings, International Snow Science Workshop, Snowbird, Utah, October 31 to November 2, p.260-279.

Tarboton, D. G., T. H. Jackson, J. Z. Liu, C. M. U. Neale, K. R. Cooley and J. J. McDonnell, (1995),"A Grid Based Distributed Hydrologic Model: Testing Against Data from Reynolds Creek Experimental Watershed," in Preprint Volume, American Meteorological Society Conference on Hydrology, Dallas, Texas, January 15-20, p.79-84.

Toews, D. A. A. and D. R. Guns, (1988),"Translating snow hydrology research results into guidelines for forest managers; gaps between theory and practice," in 56th Annual Meeting, Western Snow Conference, Kalispell, Montana, April 19-21, p.13-34.

Troendle, C. A. and C. F. Leaf, (1981),"Effects of Timber Harvest in the Snow Zone on Volume and Timing of Water Yield," in Interior West Watershed Management Symposium, Spokane, Washington, p.231-343.

U.S. Army Corps of Engineers, (1956), "Snow Hydrology, Summary report of the Snow Investigations," , U.S. Army Corps of Engineers, North Pacific Division, Portland, Oregon.

Verstraete, M. M., (1987a), "Radiation Transfer in Plant Canopies: Scattering of Solar Radiation and Canopy Reflectance," Journal of Geophysical Research, 93(D8): 9483-9494.

Verstraete, M. M., (1987b), "Radiation Transfer in Plant Canopies: Transmission of Direct Solar Radiation and the Role of Leaf Orientation," Journal of Geophysical Research, 92(D9): 10985-10995.

Verstraete, M. M., B. Pinty and R. E. Dickinson, (1990), "A physical model of the bidirectional reflectance of vegetation canopies, 1. Theory," Journal of Geophysical Research, 95(D8): 11755-11765.

Viessman, W., G. L. Lewis and J. W. Knapp, (1989), Introduction to Hydrology, 3rd Edition, Harper & Row.

Wiscombe, W. J. and S. G. Warren, (1981), "A Model of the Spectral Albedo of Snow. I: Pure Snow," Journal of the Atmospheric Sciences, 37: 2712-2733.

World Meteorological Organization, (1986), "Intercomparison of models of snowmelt runoff," Operational Hydrology Report no. 23, Publication no. 646, World Meteorological Organization.

Young, R. A., G. R. Benoit and C. A. Onstad, (1989), "Snowmelt and frozen soil," Chapter 3 in USDA Water Erosion Prediction Project, Hillslope profile model documentation, Edited by L. J. Lane and M. A. Nearing, NSERL Report #2, USDA-ARS National Soil Erosion Research Laboratory, West Lafayette, Indiana, 47907.

Figure Captions

Figure 1. Energy fluxes involved in snowmelt and snowpack ablation.

Q_{sn} - Net Solar radiation
Q_{ln} - Net longwave radiation
Q_p - Heat brought with precipitation
Q_h - Sensible heat
Q_e - Latent heat of sublimation/condensation
Q_g - Ground heat flux
Q_m - Heat carried away by melt

Figure 2. Snow model physics and parameterizations

Figure 3. Depth of penetration of temperature fluctuations into soil with thermal conductivity α = 0.0018 m^2/hr.

Figure 4. Comparison between observed and modeled snow water equivalence, CSSL.

Figure 5. Comparison between observed and modeled snow surface temperatures, CSSL. Net indicates model driven by measured net radiation. Solar indicates model driven by measured solar radiation.

Figure 6. Comparison between observed and modeled net radiation, CSSL. Measured solar radiation is input.

Figure 7. Comparison between observed and modeled melt outflow rate, CSSL. Measured solar radiation is input.

Figure 8. Upper Sheep Creek topography and instrumentation

Figure 9. Weighted Average Drift factors at Upper Sheep Creek (after *Jackson,* 1994; *Jackson et al.*, 1996). Contours at 0.5, 0.9, 1.5, 2.5, 4 and 6.

Figure 10. Observed and simulated spatial distribution of snow water equivalence at Upper Sheep Creek (after *Jackson,* 1994; *Jackson et al.*, 1996).

Figure 11. 1985-6 season cumulative snowmelt measured and simulated at locations D3 and L10 (see grid on figure 8.) at Upper Sheep Creek.

Figure 12. Upper Sheep Creek area average snow water equivalence, modeled and observed. a) 1985/6, b) 1992/3. c) 1992/3. Model initialized on 3/3/93.

Figure 13. Overall snow accumulation and ablation measurements at USU research farm.

Figure 14. Observed and modeled snow water equivalence, USU research farm.

Figure 15. Comparison of measured and modeled energy content of the snow and top 0.4 m of soil at USU research farm.

Figure 16. Measured soil and snow temperatures on February 8, 1993 (day 39) at USU research farm.

Figure 17. Measured and modeled snow surface temperature for January 16 to February 7, 1993 (days 26 to 38) at USU research farm.

Figure 18. Detailed results for melt period, March 9, 1993 to March 23, 1993 (days 69 to 82) at USU research farm.

Figure 18. Detailed results for melt period, March 9, 1993 to March 23, 1993 (days 69 to 82) at USU research farm continued.

Figure 19. Snow water equivalence (SWE) observed at Mammoth Mountain snow pits compared to modeled.

Figure 20. Mammoth Mountain south lysimeter cluster discharge compared to modeled.

Figure 21. Mammoth Mountain north lysimeter cluster discharge compared to modeled.

Figure 22. Mammoth Mountain calculated and observed albedo.

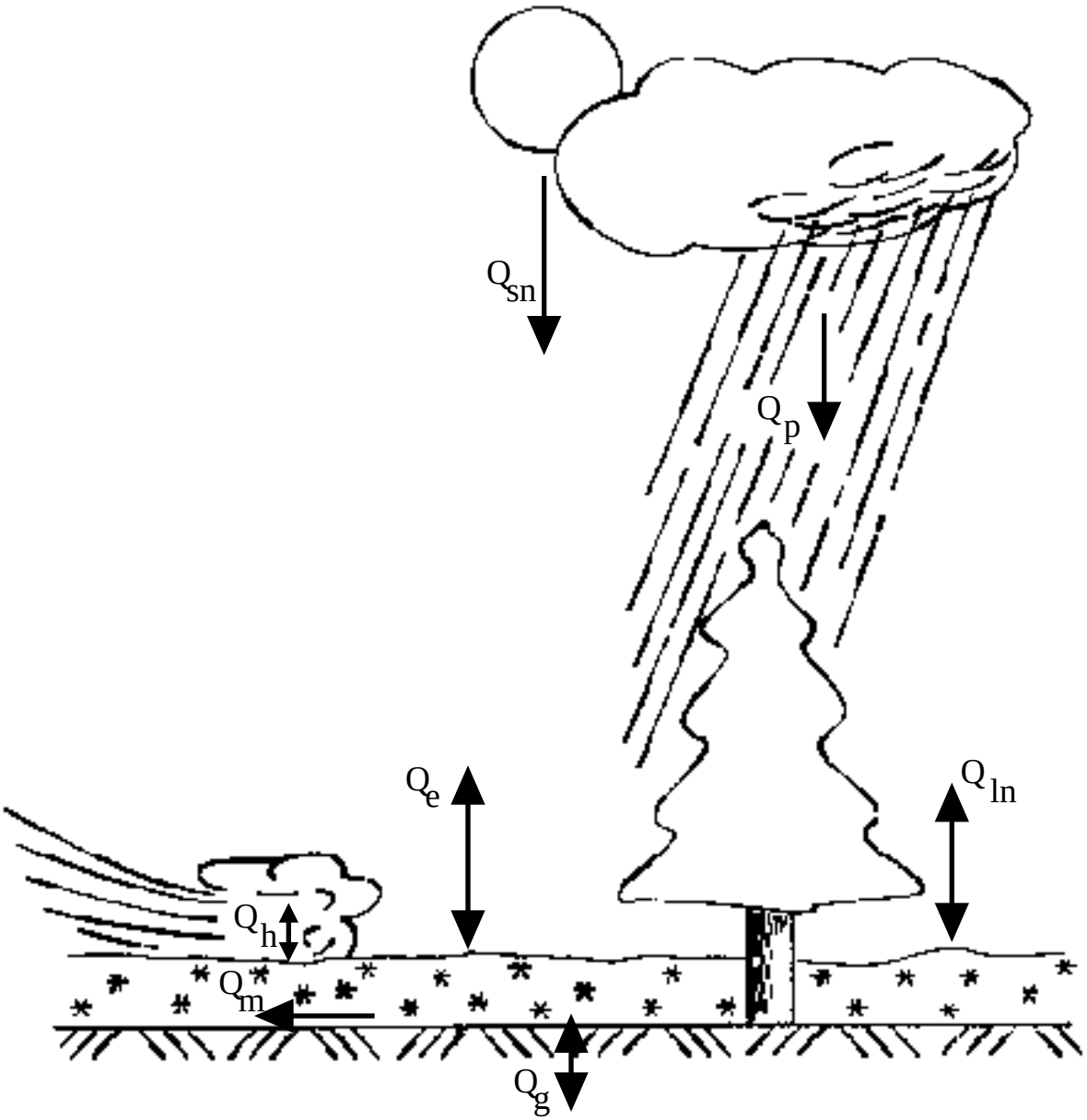

Figure 1. Energy fluxes involved in snowmelt and snowpack ablation.

Q_{sn}- Net Solar radiation
Q_{ln}- Net longwave radiation
Q_p - Heat brought with precipitation
Q_h - Sensible heat
Q_e - Latent heat of sublimation/condensation
Q_g - Ground heat flux
Q_m- Heat carried away by melt

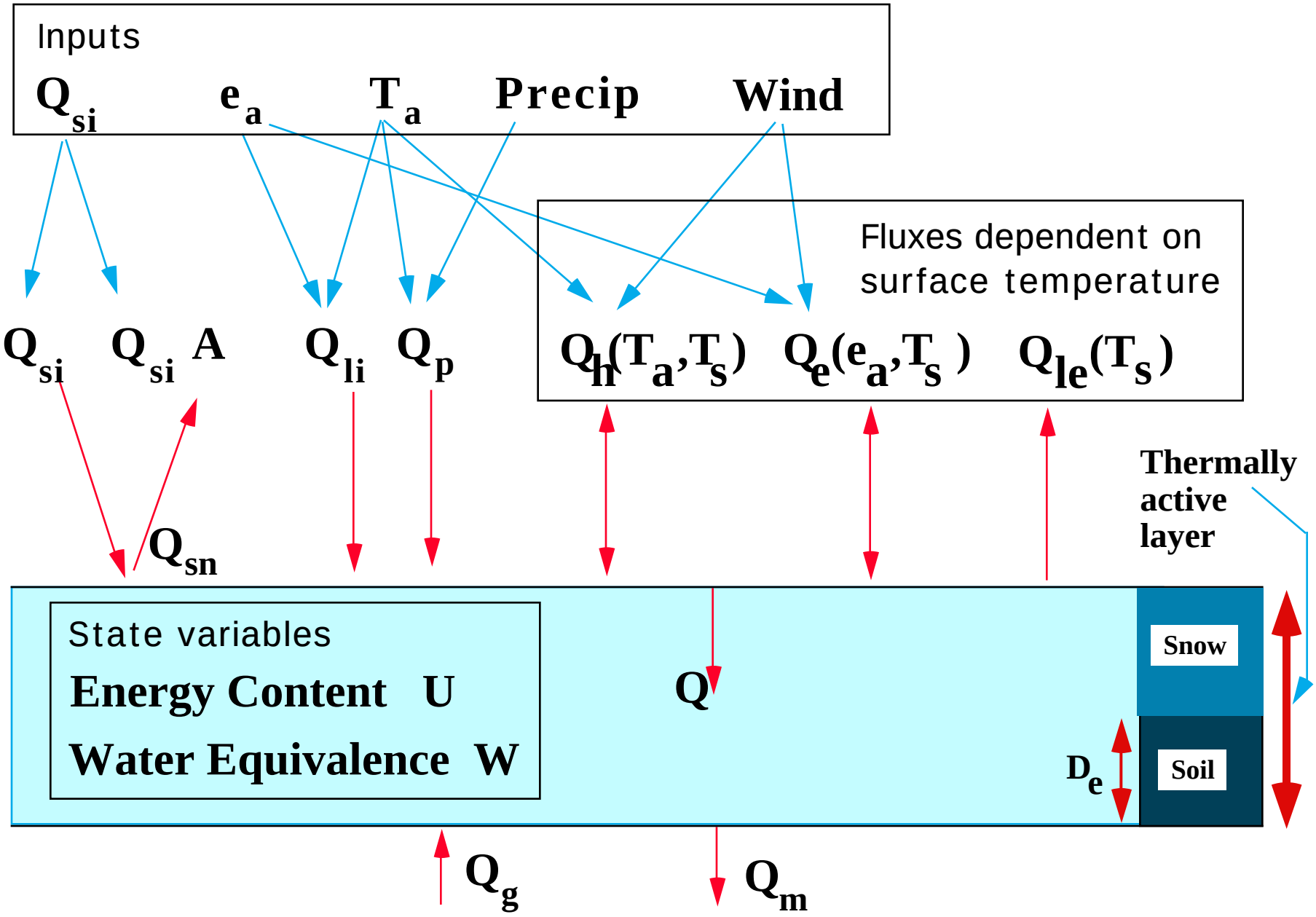

Figure 2. Snow Model Physics and Parameterizations

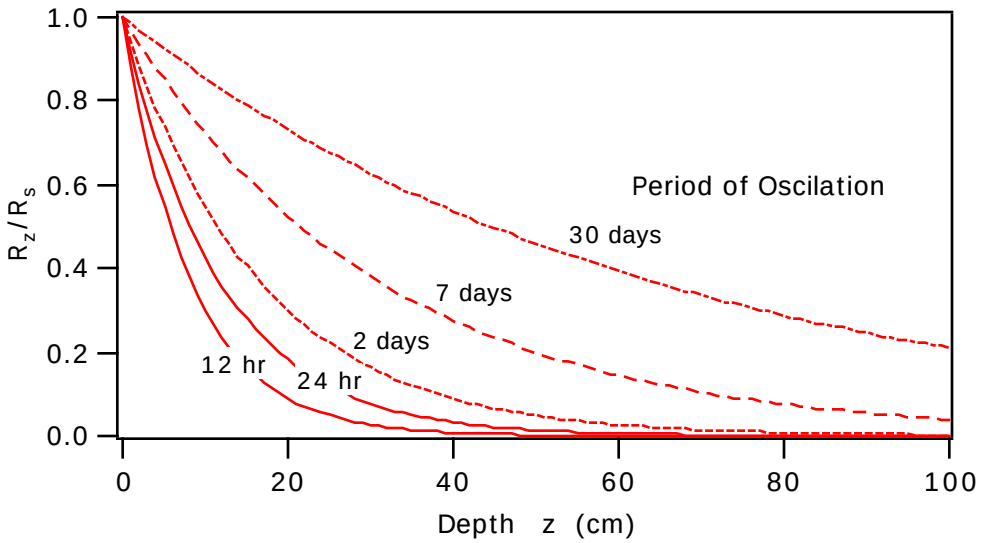

Figure 3. Depth of penetration of temperature fluctuations into soil with thermal conductivity α = 0.0018 m^2/hr.

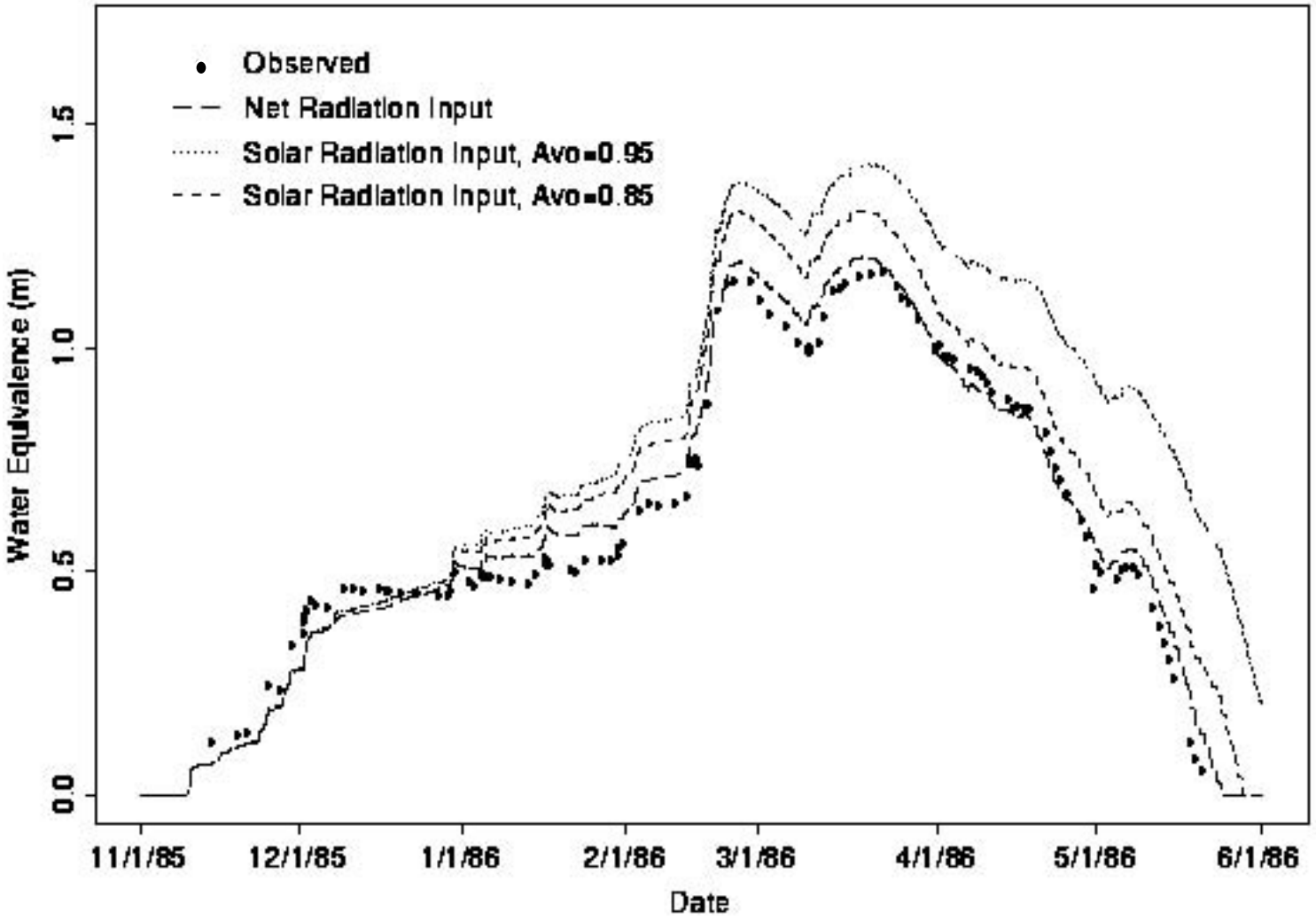

Figure 4. Comparison between observed and modeled snow water equivalence, CSSL.

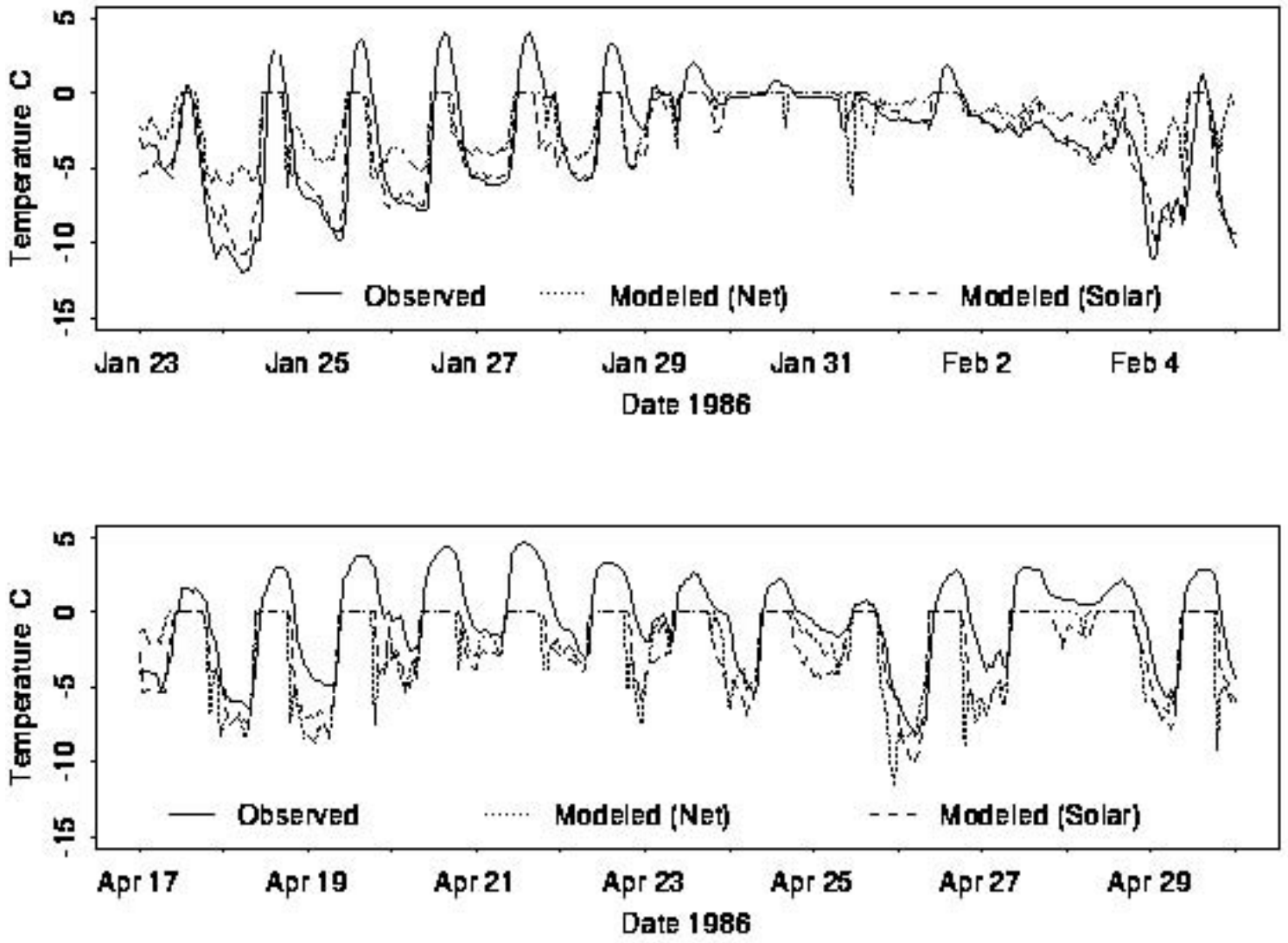

Figure 5. Comparison between observed and modeled snow surface temperatures, CSSL. Net indicates model driven by measured net radiation. Solar indicates model driven by measured solar radiation.

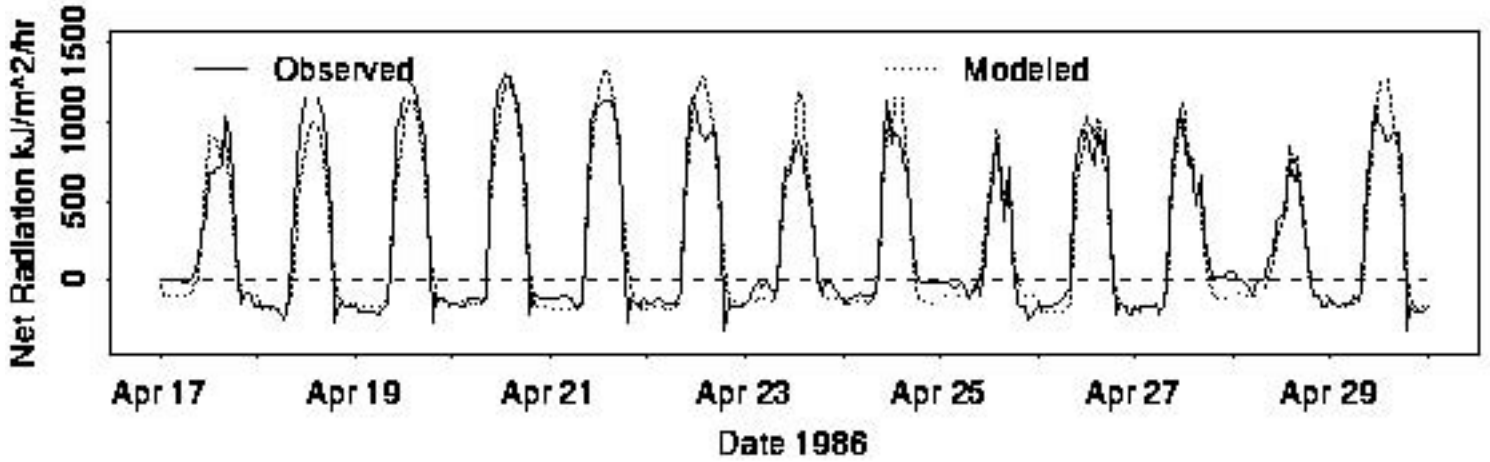

Figure 6. Comparison between observed and modeled net radiation, CSSL. Measured solar radiation is input.

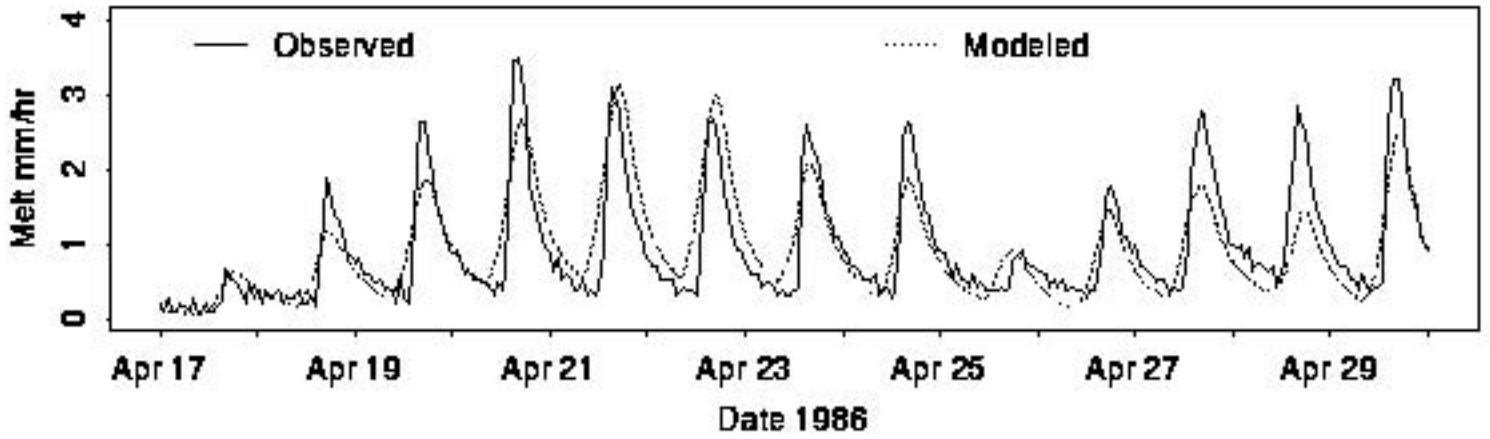

Figure 7. Comparison between observed and modeled melt outflow rate, CSSL. Measured solar radiation is input.

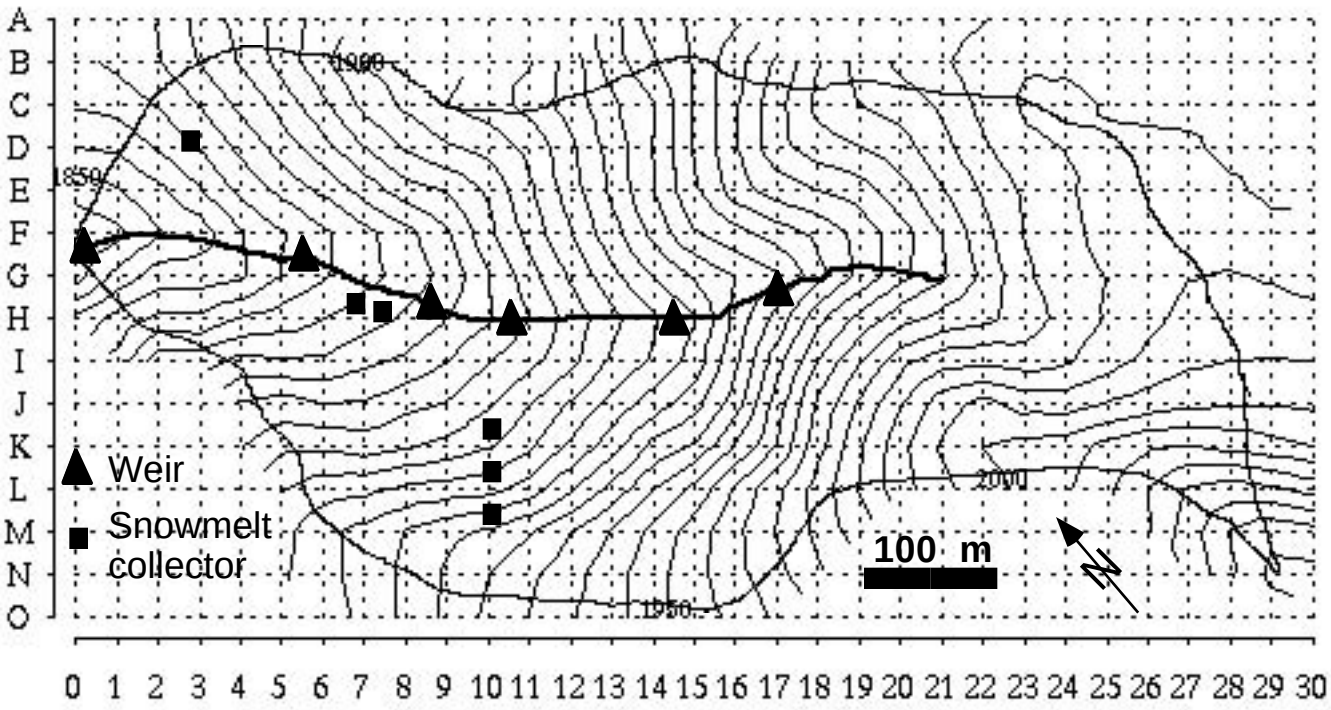

Figure 8. Upper Sheep Creek topography and instrumentation

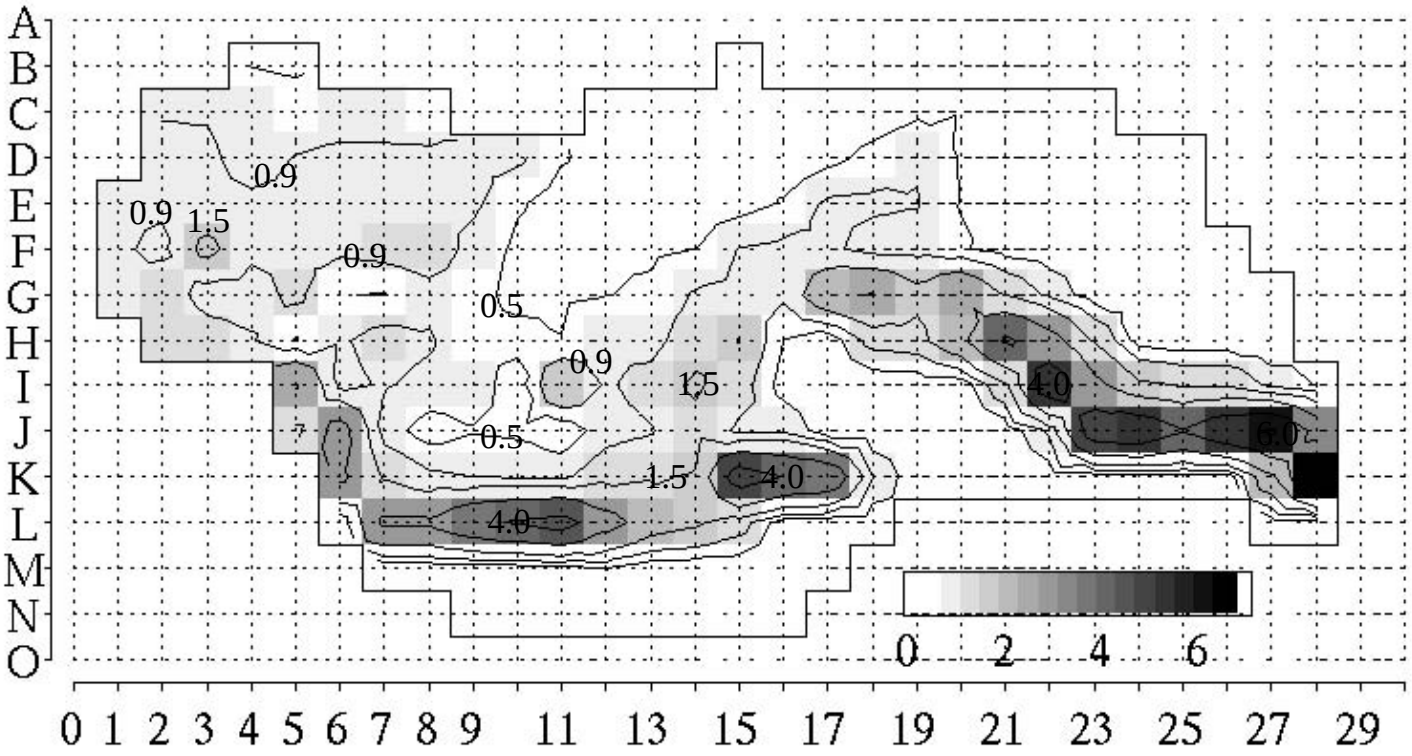

Figure 9. Weighted Average Drift factors at Upper Sheep Creek [after \Jackson, 1994 #1663; Jackson, 1996]. Contours at 0.5, 0.9, 1.5, 2.5, 4 and 6.

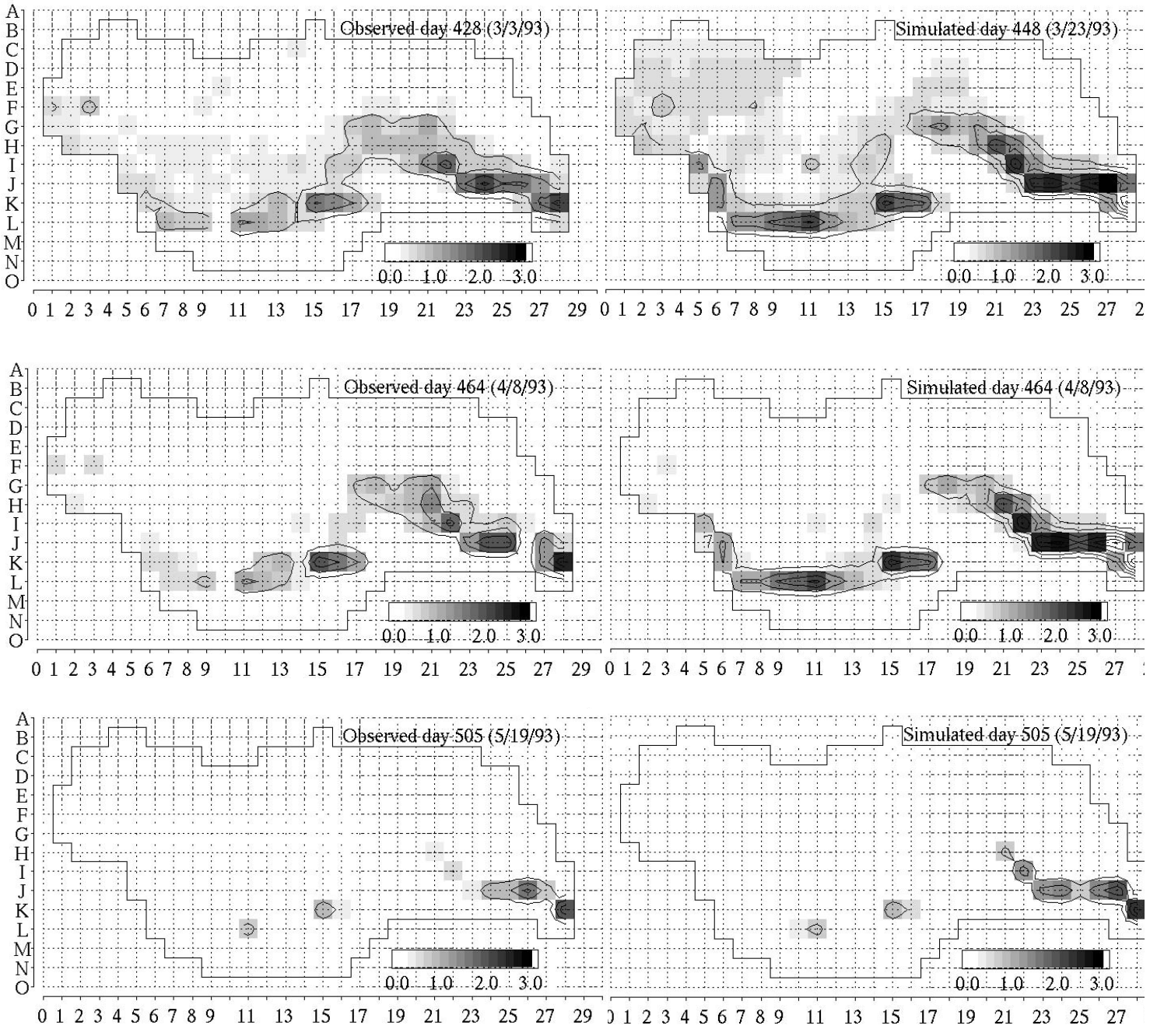

Figure 10. Observed and simulated spatial distribution of snow water equivalence at Upper Sheep Creek (after *Jackson*, 1994; *Jackson et al.*, 1996).

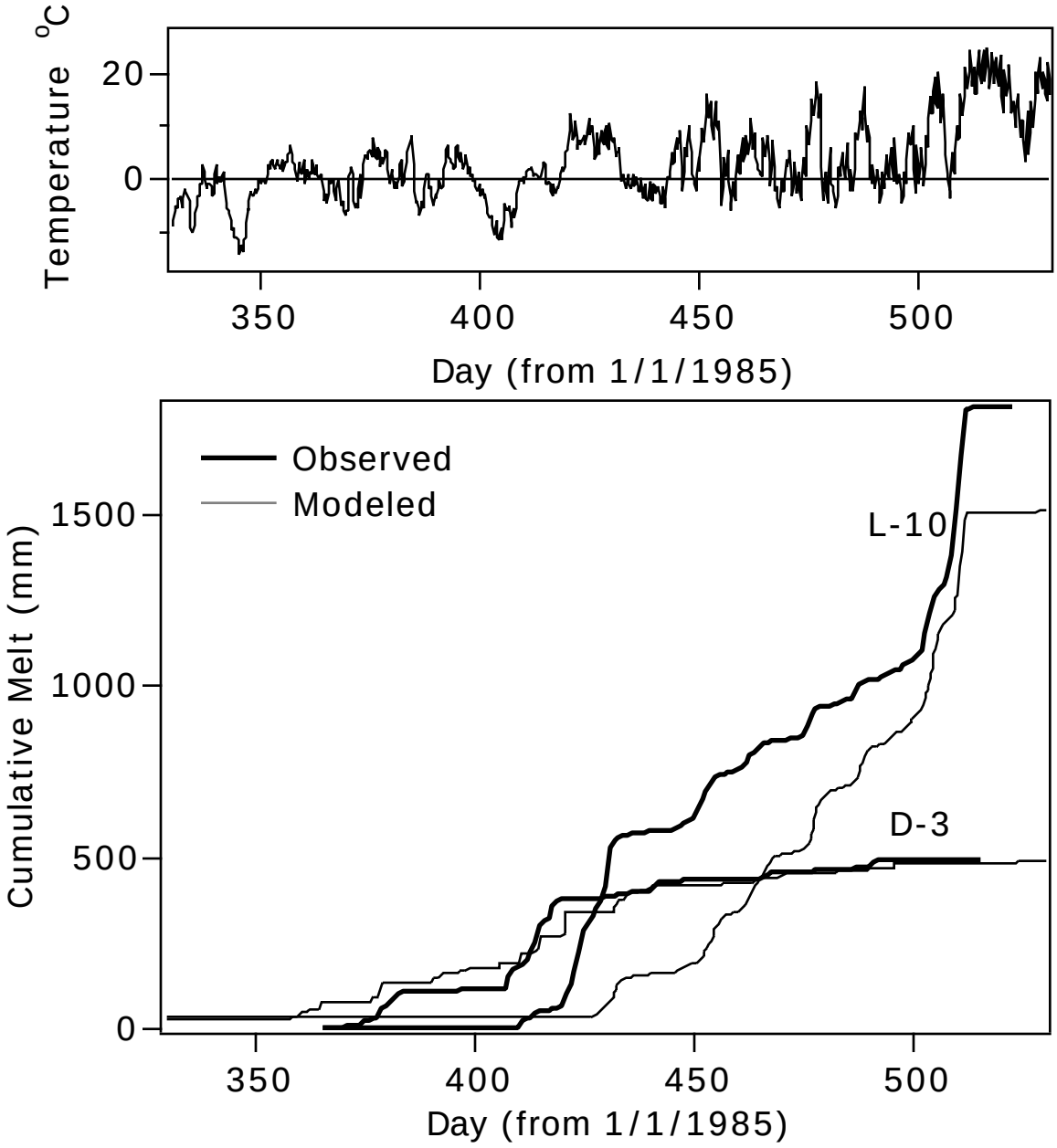

Figure 11. 1985-6 season cumulative snowmelt measured and simulated at locations D3 and L10 (see grid on figure 8.) at Upper Sheep Creek.

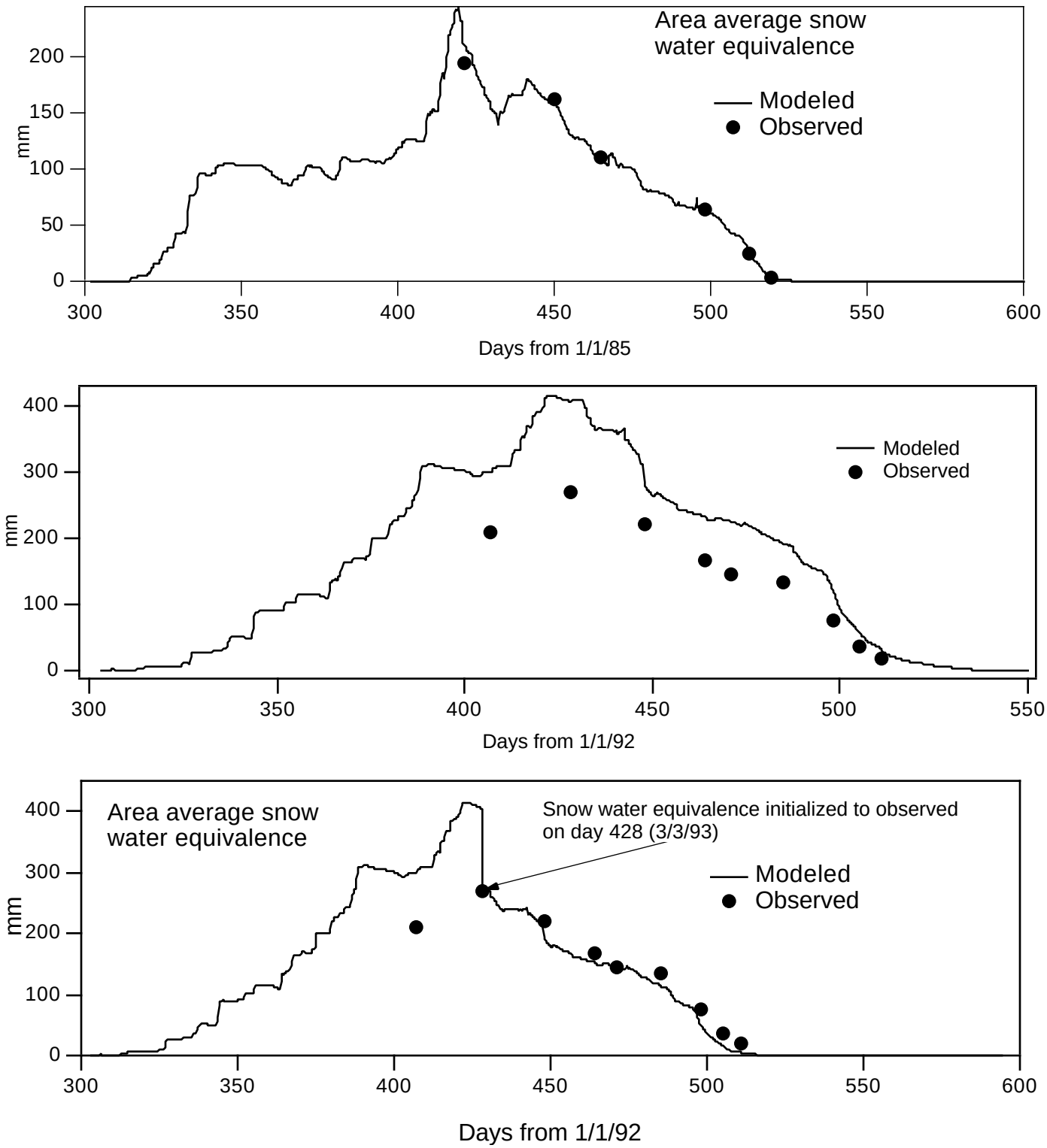

Figure 12. Upper Sheep Creek area average snow water equivalence, modeled and observed. a) 1985/6, b) 1992/3. c) 1992/3. Model initialized on 3/3/93.

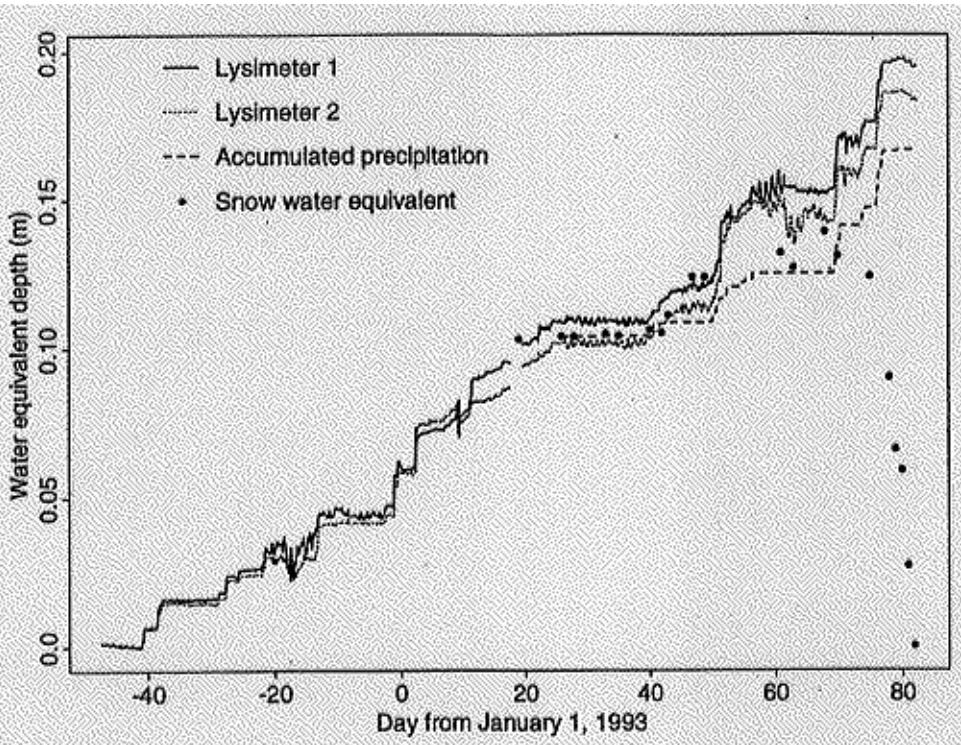

Figure 13. Overall snow accumulation and ablation measurements at USU research farm.

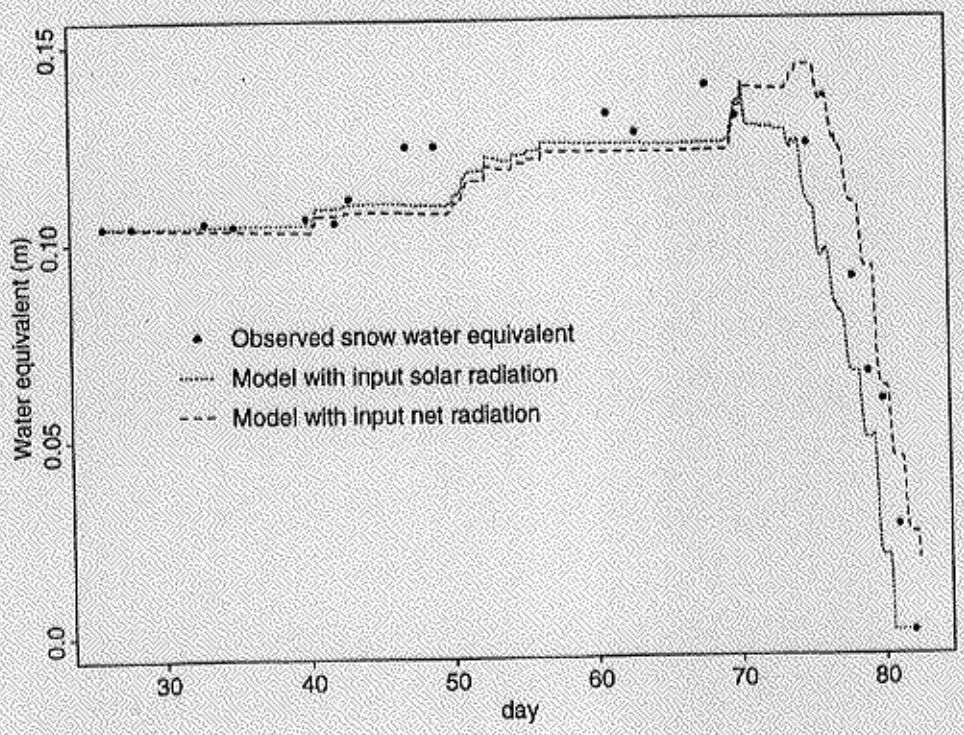

Figure 14. Observed and modeled snow water equivalence, USU research farm.

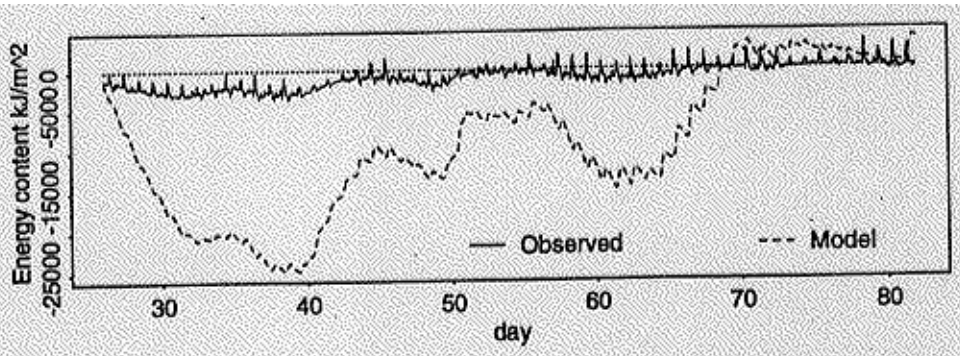

Figure 15. Comparison of measured and modeled energy content of the snow and top 0.4 m of soil at USU research farm.

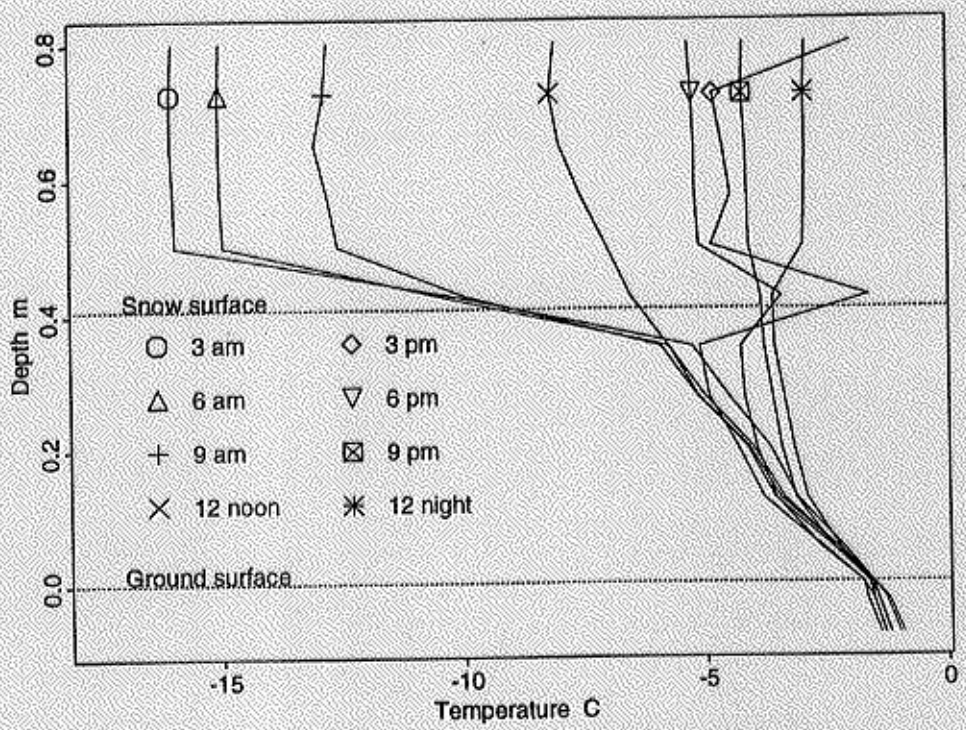

Figure 16. Measured soil and snow temperatures on February 8, 1993 (day 39) at USU research farm.

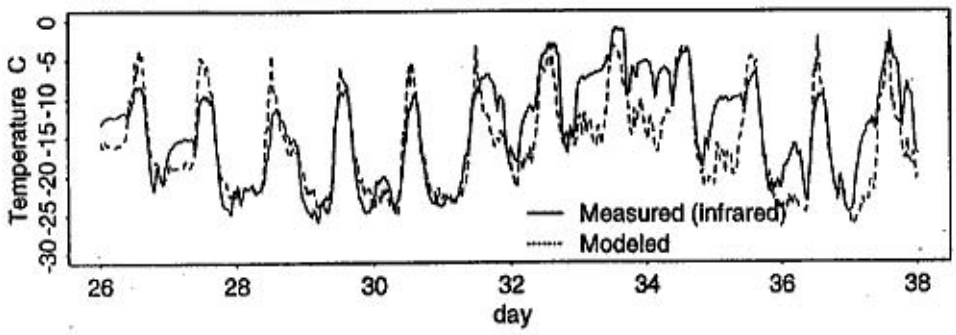

Figure 17. Measured and modeled snow surface temperature for January 16 to February 7, 1993 (days 26 to 38) at USU research farm.

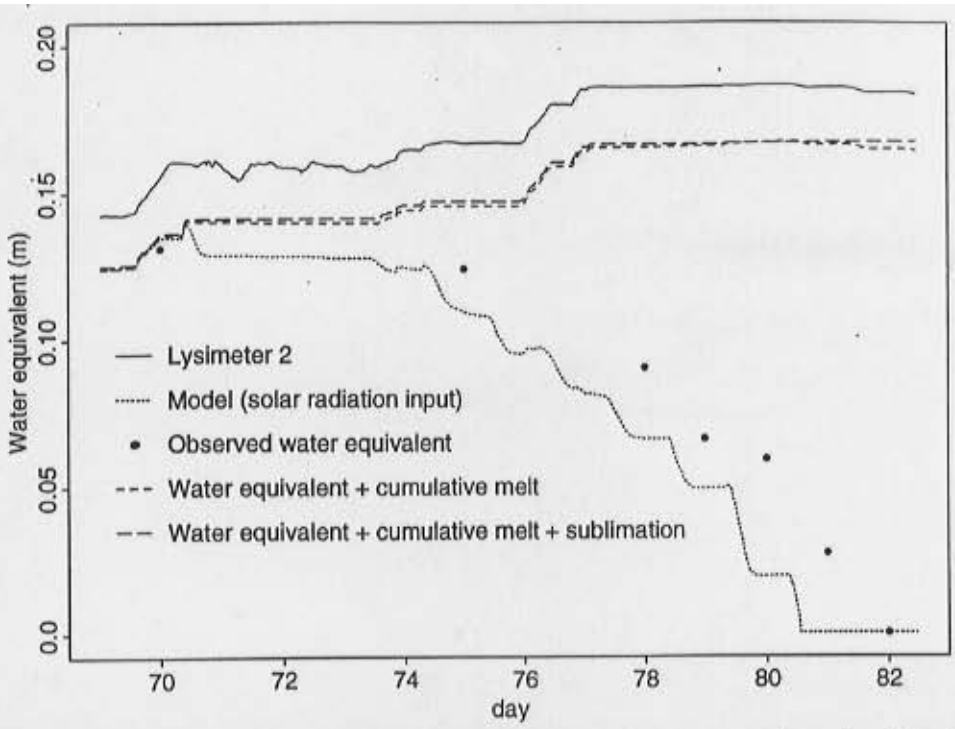

a) Lysimeter, modeled and measured snow water equivalent, accumulated melt and sublimation.

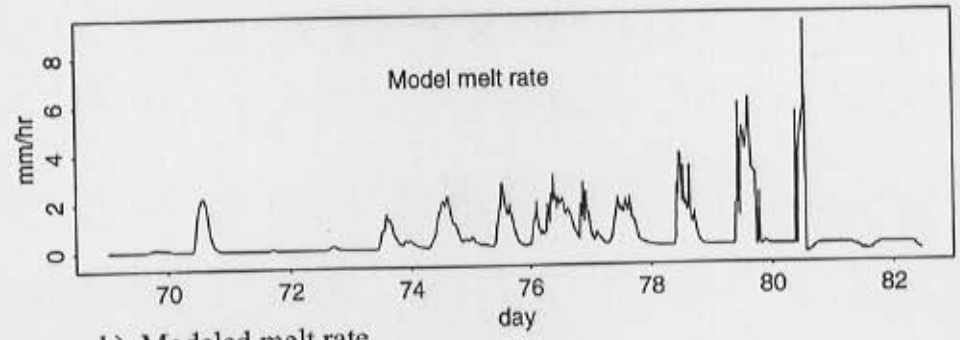

b) Modeled melt rate.

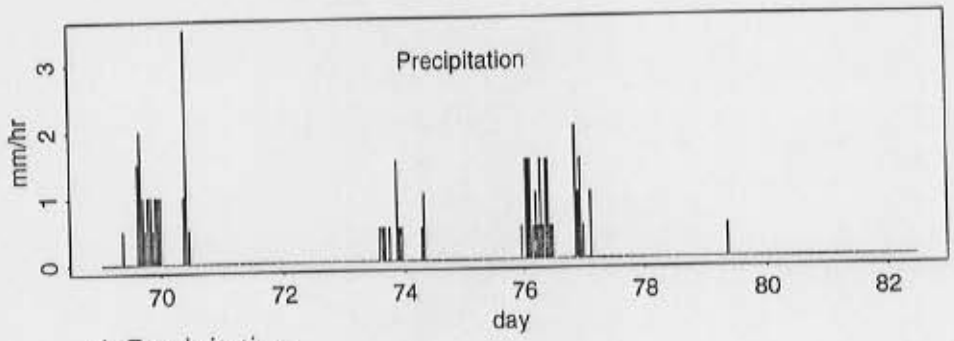

c) Precipitation.

Figure 18. Detailed results for melt period, March 9, 1993 to March 23, 1993 (days 69 to 82) at USU research farm.

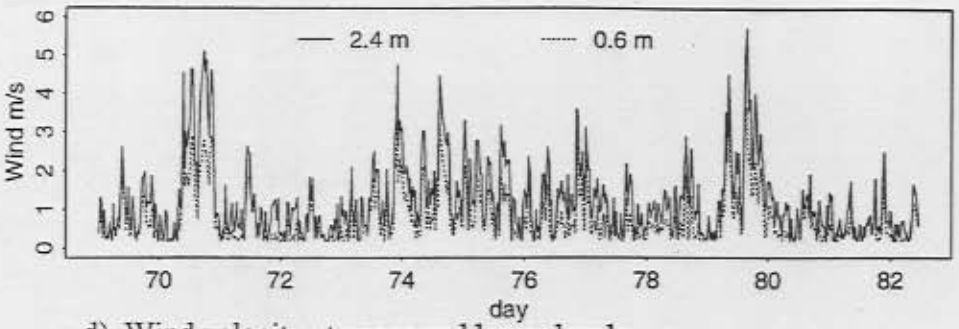

d) Wind velocity at upper and lower levels

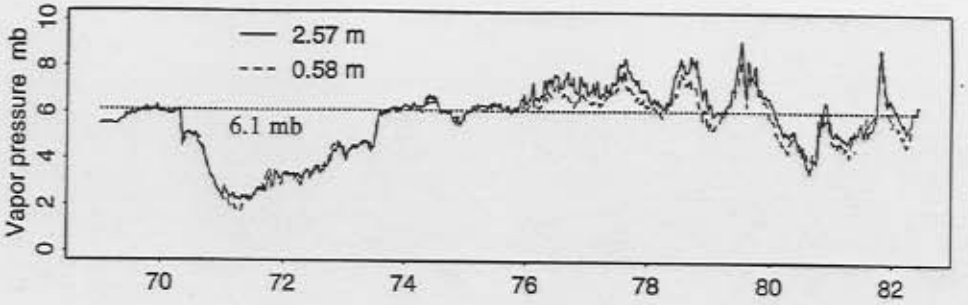

g) Water vapor pressure at upper and lower levels.

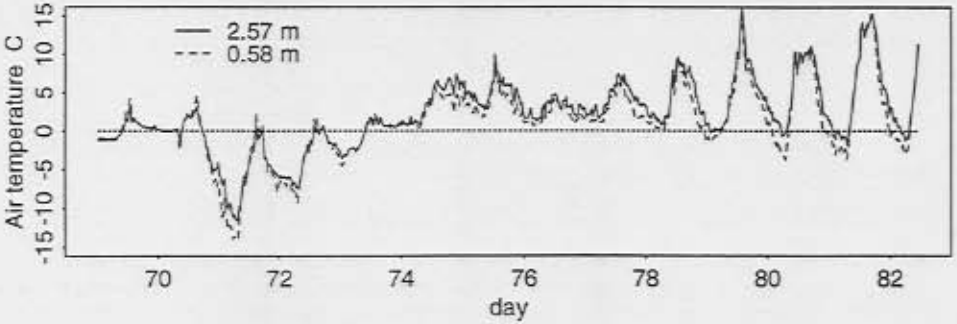

e) Air temperature at upper and lower levels.

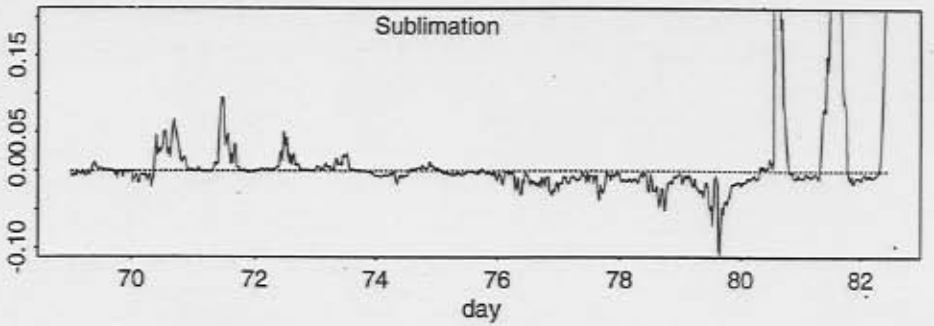

h) Modeled sublimation.

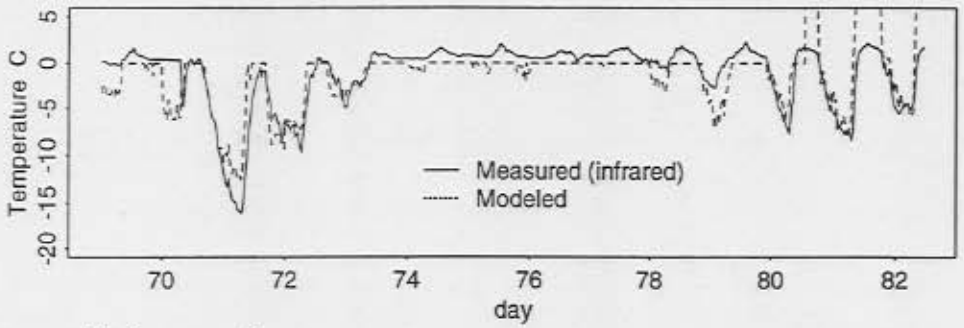

f) Snow surface temperature.

Figure 18. Detailed results for melt period, March 9, 1993 to March 23, 1993 (days 69 to 82) at USU research farm continued.

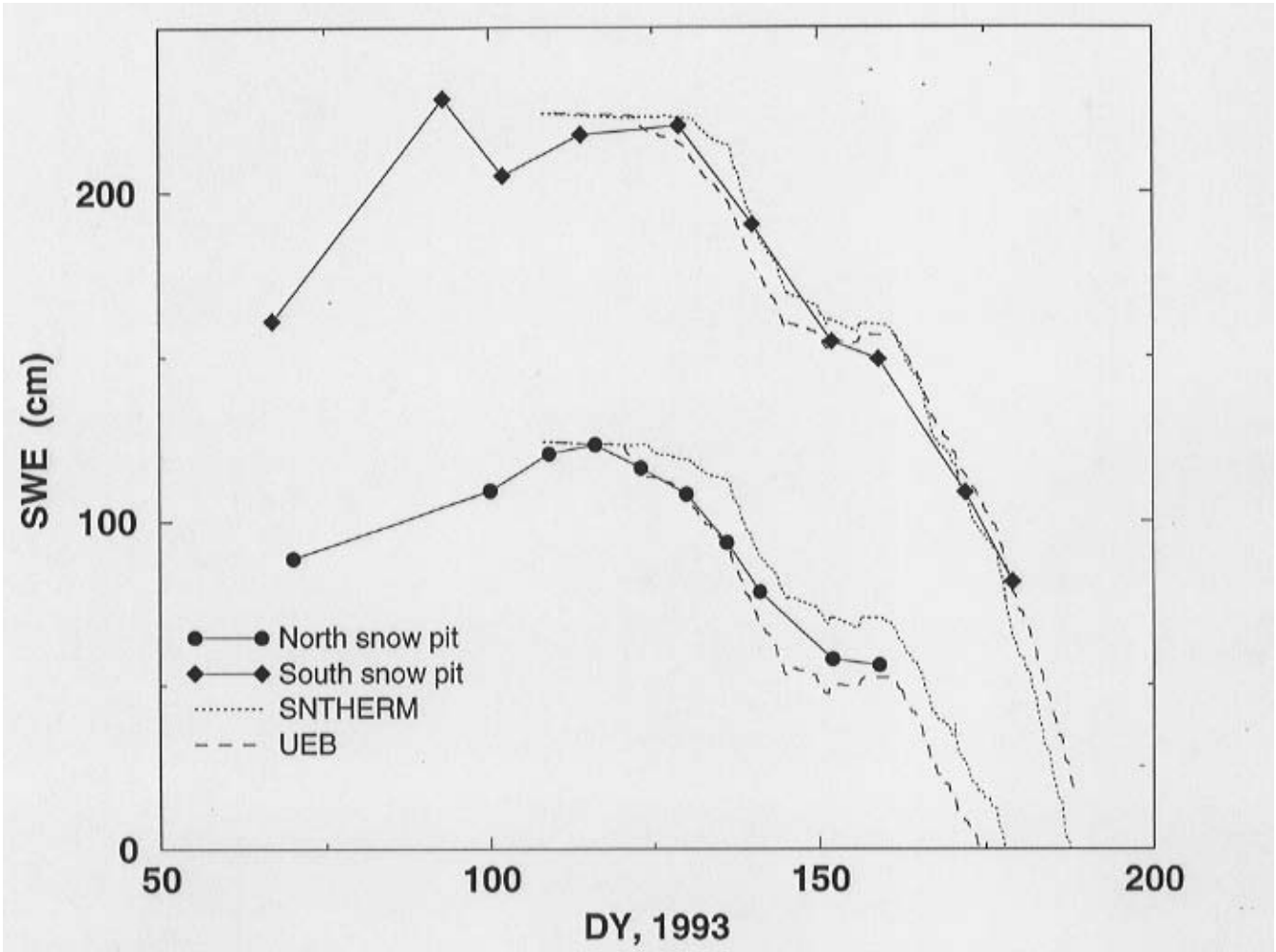

Figure 19. Snow water equivalence (SWE) observed at Mammoth Mountain snow pits compared to modeled.

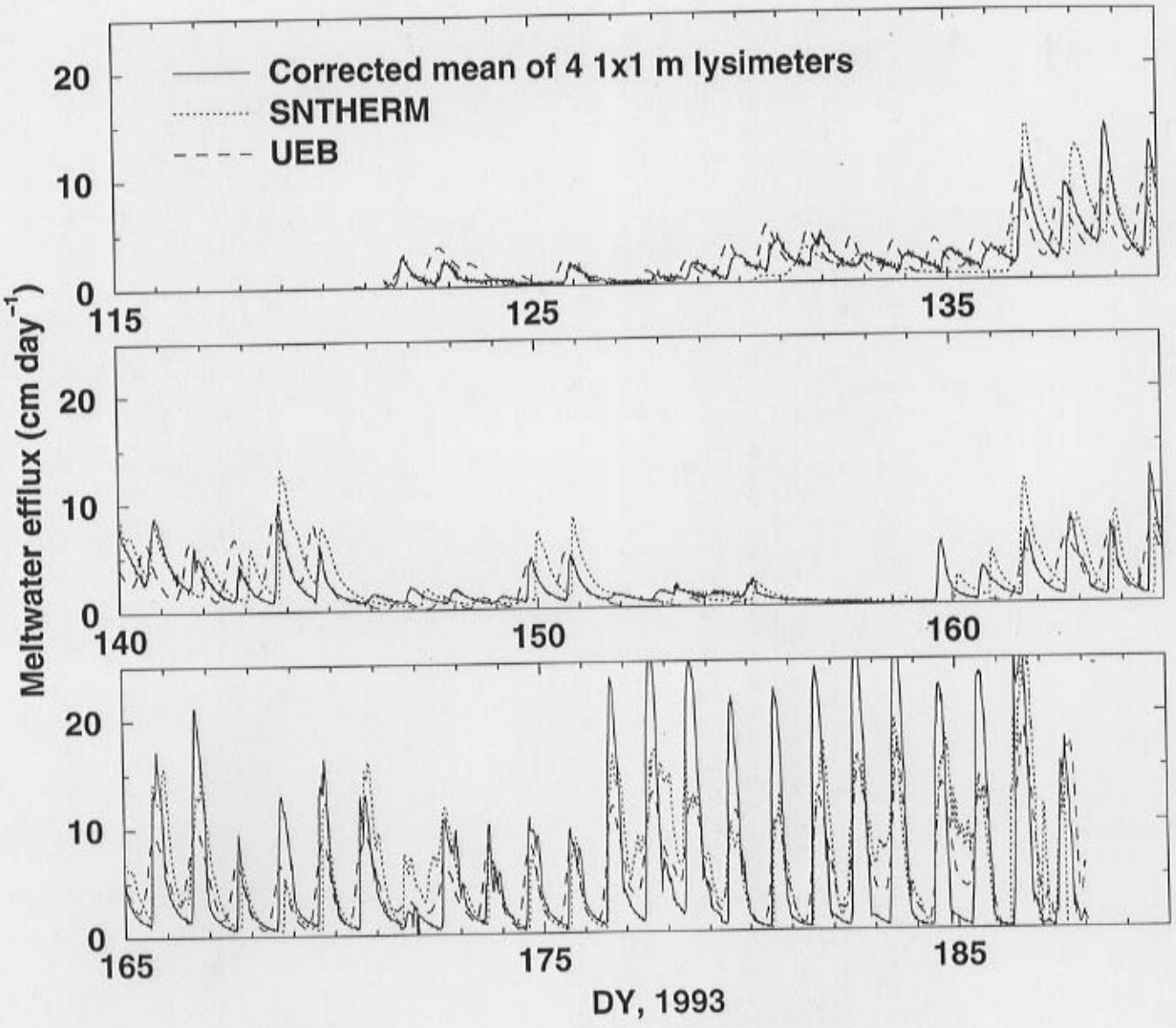

Figure 20. Mammoth Mountain south lysimeter cluster discharge compared to modeled.

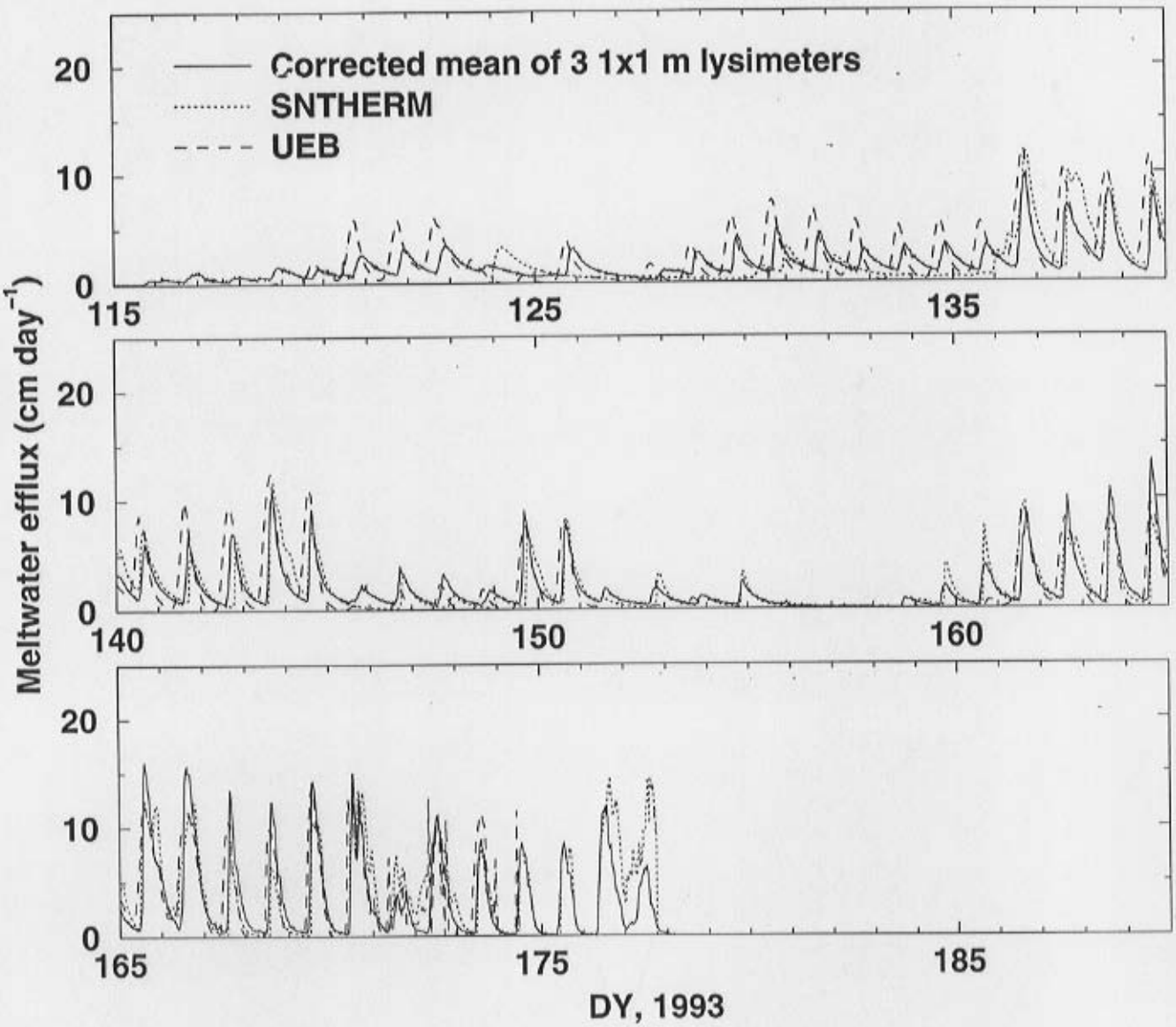

Figure 21. Mammoth Mountain north lysimeter cluster discharge compared to modeled.

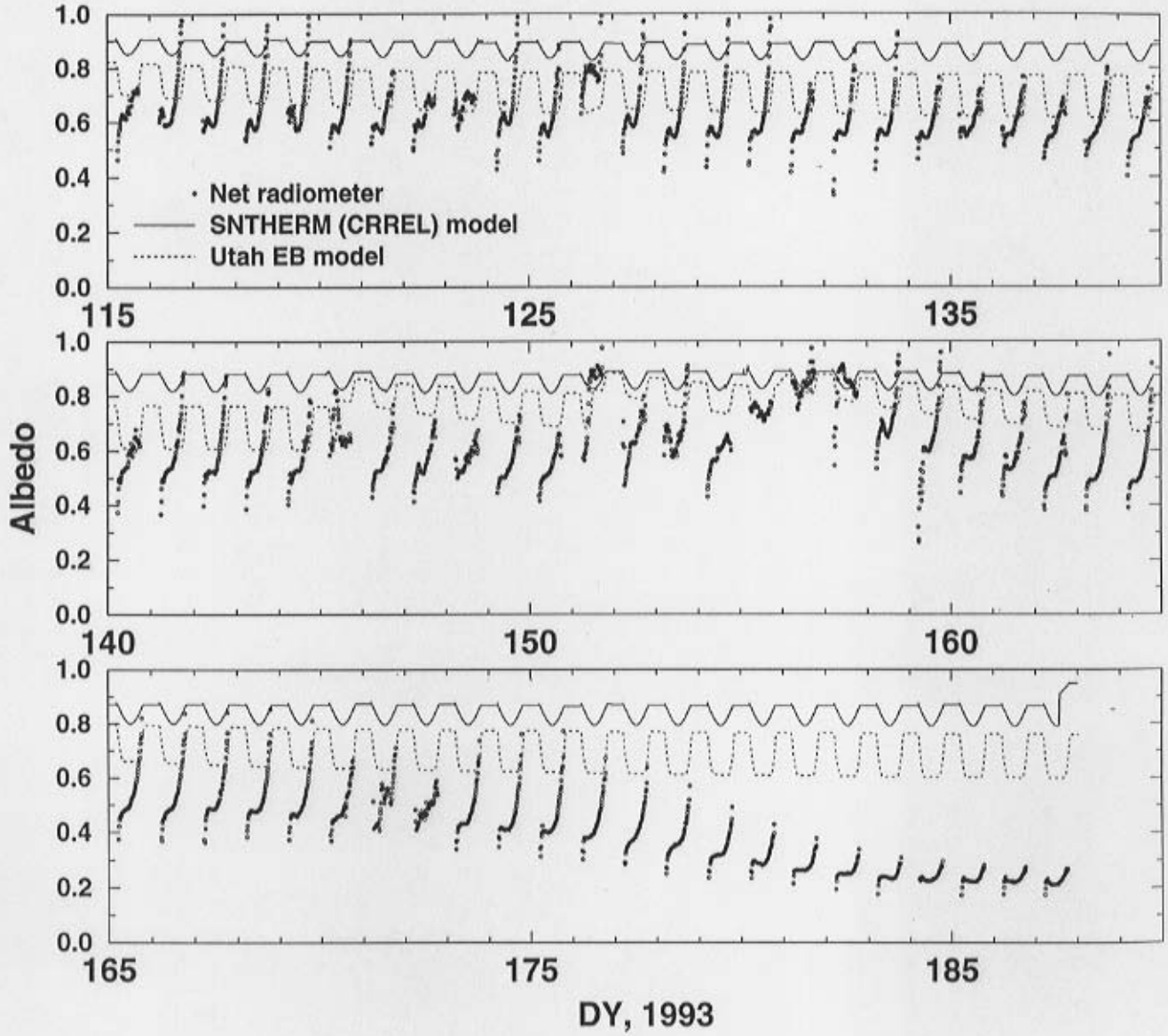

Figure 22. Mammoth Mountain calculated and observed albedo.